FOREX Publication
Open Access | Rapid and quality publishing

International Journal of
Electrical and Electronics Research (IJEER)
Research Article | Volume 12, Issue 4 | Pages 1301-1323 | e-ISSN: 2347-470X

Hybrid Learning Approach for Automated Identification and Categorization of Cardiovascular Disorders

Padmavathi C[1*] and Veenadevi S V[2]

[1]*Research Scholar, Electronics and Communication Engineering, Visvesvaraya Technological University, Belagavi, Karnataka, India; padmavathic87@gmail.com*
[2]*Associate Professor, R V College of Engineering, Electronics and Communication Engineering, Visvesvaraya Technological University, Belagavi, Karnataka, India; veenadevi@rvce.edu.in*

*__Correspondence:__ Padmavathi C; *padmavathic87@gmail.com*

ABSTRACT- Cardio Vascular Diseases (CVDs) pose an important global health challenge, contributing substantially to mortality rates worldwide. Electrocardiography (ECG) is a necessary diagnostic tool in the detection of CVDs. Manual analysis by medical experts, for ECG interpretation, is laborious and subject to interobserver variability. To overcome these limitations, automated categorization technique has gained prominence, enabling efficient CVDs classification. The major focus of this work is to utilize deep learning (DL) approach for the identification of CVDs using ECG signals. The presented work incorporates two hybrid models: one-dimensional convolutional neural network (1D-CNN) with Recurrent Hopfield Neural Network (1D-CNN-RHNN) and with Residual Network (1D-CNN-ResNet), to obtain important features from raw data and categorize them into different groups that correlate to CVD situation. The 1D-CNN-RHNN model achieved classification accuracy of 96.62% in the 4-class classification of normal, coronary artery disease (CAD), myocardial infarction (MI), and congestive heart failure (CHF) and the 1DCNN-ResNet model achieved classification accuracy of 95.75% in the 5-class classification of normal, CAD, MI, CHF and cardiomyopathy. The proposed model's functionality is validated with medical ECG data, and its outcomes are evaluated using various measures. Experimental findings demonstrate that the proposed models outperform other existing approaches in categorizing multiple classes. Our suggested approach might potentially help doctors screen for CVDs using ECG signals and is capable of being verified with larger databases.

Keywords: Cardiovascular disease; Electrocardiogram; Convolutional neural network; Residual neural network; Recurrent hop field neural network.

ARTICLE INFORMATION

Author(s): Padmavathi C and Veenadevi S V;
Received: 03/07/2024; **Accepted**: 10/10/2024; **Published**: 30/11/2024;
e-ISSN: 2347-470X;
Paper Id: IJEER 0307-06;
Citation: 10.37391/ijeer.120423
Webpage-link:
https://ijeer.forexjournal.co.in/archive/volume-12/ijeer-120423.html

Publisher's Note: FOREX Publication stays neutral with regard to Jurisdictional claims in Published maps and institutional affiliations.

1. INTRODUCTION

According to the World Health Organization (WHO), CVDs would likely take responsibility for 19.1 million deaths worldwide in 2020 [1]. ECG (*Figure 1*) is a widely employed non-invasive tool for diagnosing CVDs by providing real-time electro-physical measurements of cardiac activities, reflecting the working state of the heart. The interpretation of ECG signals poses significant challenges in detecting and diagnosing various cardiovascular conditions. It has ability to detect arrhythmias [2] assess myocardial damage, evaluate cardiac morphology, identify conduction disturbances [3] and monitor treatment efficacy. ECG provides clinicians with valuable insights into abnormal cardiac rhythms, myocardial ischemia, cardiac chamber enlargement, conduction system abnormalities, and the effectiveness of therapeutic interventions. When combined with other clinical assessments, ECG facilitates comprehensive and scientifically informed decision-making in the management of CVDs.

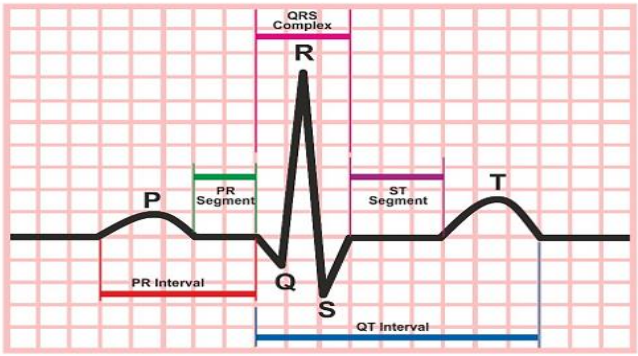

Figure 1. ECG waveform

A full evaluation of the heart's electrical activity from various perspectives is provided by acquiring a complete ECG employing 10 electrodes to record 12 leads. Although all 12 leads are essential for accurate diagnosis, a single lead, particularly lead II, can provide significant initial assessment information. The five unique waves that make up an ECG cycle made of P, Q, R, S, and T- reflecting different stages of the heart's activity. The T-wave should coincide with the QRS complex [4]. The left ventricle mostly contributes to the

FOREX Publication
Open Access | Rapid and quality publishing
International Journal of Electrical and Electronics Research (IJEER)
Research Article | Volume 12, Issue 4 | Pages 1301-1323 | e-ISSN: 2347-470X

waveform, and the P-wave represents the initial positive deflection. Activity of the ventricles (left and right) is reflected by the QRS complex. In contrast, the P-R interval measures the amount of time between the start of the P-wave and the first deflection of the QRS complex. For instance, the Q-T interval measures the time between the end of the T-wave at the isoelectric line and the first deflection of the QRS complex [5]. Any deviations in the functionality of the heart as a result of many types of heart ailments are depicted in the morphology as briefed in *table 1*.

Table 1. Variety of Heart Diseases and their ECG Characteristics

Heart Disease	ECG Characteristics
Coronary Artery Disease	ST-segment, T-wave inversions, pathological Q-waves
Heart Failure	Prolonged QRS duration
Valvular Heart Diseases	Changes in QRS complex shape or duration
Congenital Heart Defects	Abnormal ventricular hypertrophy, QRS axis conduction
Cardiomyopathy	Ventricular hypertrophy patterns, abnormal QRS duration
Infective Endocarditis	Prolonged PR intervals, heart block, conduction disturbances
Pericardial Diseases	ST-segment elevations, PR-segment depressions
Arrhythmias	Irregular rhythms, characteristic waveform changes

Advanced methods have surpassed traditional methods in the accurate and quick identification of cardiac disorders through the use of automated models and the extraction of pertinent information from ECG data. The automated classification of cardiovascular illnesses using artificial intelligence has shown promise, offering the potential to revolutionize diagnosis and treatment [6]. One notable advantage of AI-based approaches is their ability to process vast amounts of data rapidly and accurately, surpassing human capabilities in terms of speed and consistency [7]. Classical predictive algorithms necessitate gathering features in advance of usage, which entails gathering many handmade elements affecting sorting results. The laborious extraction of features procedure with the manually performed utilization of signals anatomy, as well as the development of the feature design manage is lengthy, neglects the basic data in the repository, while is vulnerable to problems with over-fit the ability to adapt fails in the case from evolving ECG patterns and noticeable disruption. Various elements effect the way they perform, notably characteristic recognition, extractor approaches, neural networks for classification, and assessment using biased information. Such traits may reduce the ability to recognize effectiveness of the minority class, indicating the demand to keep improving with such structures. Emergence in DL opens up exciting possibilities towards tackling this challenge. DL improves grouping frameworks' efficacy as well as adaptability through acquiring excellent high degree of data without delay.

In recent years, DL approaches for classification have emerged, which can analyze ECG signals in real-time, enabling the swift detection of abnormalities and facilitating timely interventions. The integration of DL into the management of CVDs holds several significant benefits. Firstly, it enhances the accuracy of disease detection, minimizing the risk of misdiagnosis. This improvement contributes to enhanced patient safety and helps avoid unnecessary medical interventions which automate repetitive tasks, enabling healthcare professionals to focus on complex decision-making and patient care [8]. The adoption of automated methods in CVD diagnosis comes with its own set of challenges. With this it is difficult to grasp the underlying decision-making process, and the comprehensibility of models continue to be major challenges. In order to increase confidence between medical professionals and automated systems, efforts are being made to build explainable automated learning techniques that offer insights into the thinking behind automated models.

The ability to predict multiple heart diseases through DL expands the scope of diagnostic capabilities, which holds significant implications for comprehensive cardiac assessment, personalized treatment strategies, and improved patient care, reducing the burden on healthcare professionals. However, this field faces limitation pertaining to the complexity of CVDs, the need for diverse datasets, and the interpretability of DL algorithms. Addressing these challenges is crucial for developing an effective clinical system. Further a potential research gap exists in the development of comprehensive deep-learning models that can effectively detect and classify multiple heart diseases simultaneously. Existing studies have primarily focused on individual heart diseases or specific combinations, and there is a need for research that explores the detection of a broader range of heart diseases within a single model. This highlights the pressing need to develop more accurate and efficient models specifically designed for predicting multiple heart diseases using ECG.

We created an ECG classification mechanism using hybrid neural network inspired by previous developments in the field. The present study makes important findings in each of these sectors:

1. DL framework which negates the need of an additional feature extracting procedure is put forth. However, it constantly uses DL algorithms to derive robust characteristics using the given ECG wave. It allows for immediate conditioning and categorization of the transformed ECG, which reduces identification costs.

2. For addressing dataset inequalities, we made use of combined testing strategies. Most groups acquired lower selection, though some endured excess sampling. It normalized the available data, reducing the number of samples differences between all of the cardiac groups therefore enhancing the precision of classification.

3. We devised an application method which is a combination of 1D CNN with RHNN and 1D CNN with ResNet to extract attributes from signals, resulting in comprehensive ECG signal

FOREX Publication
Open Access | Rapid and quality publishing
International Journal of Electrical and Electronics Research (IJEER)
Research Article | Volume 12, Issue 4 | Pages 1301-1323 | e-ISSN: 2347-470X

sorting with improved effectiveness in predicting. It boosts efficacy as well as reduces the framework's structure.

2. RELATED WORK

Particle swarm optimization (PSO) based emotional neural network (EmNN) is proposed for diagnosing CAD [9]. Their model, incorporating 4 selection methods to choose features on the Z-Alizadeh sani dataset, demonstrated improved performance. Comparisons with previous efforts revealed that the accuracy, F1-score of 88.34% and 92.12% obtained were competitive. However, despite these advancements, challenges related to the limited interpretability of deep learning models, the need for large labeled datasets, and real-time implementation difficulties still persisted. One-dimensional CNN [10] approach for categorizing different cardiovascular illnesses using ECG readings employed empirical mode decomposition to break down the ECG signal and generate a modified signal for enhanced information representation, resulting in high classification accuracies of 97.70%, 99.71%, and 98.24% on three publicly available ECG databases namely MIT-BIH, St.-Petersburg, PTB respectively. However, further evaluation to validate, larger and more varied datasets is needed for the model's robustness, and real-world implementation may pose challenges due to computational complexity and preprocessing requirements. An integrated model (InRes-106) which is a combination of Inception V3 and ResNet50 that outperformed other classifiers in automated prediction of various heart ailments using ECG resulted in an accuracy of 98.34% [11]. The limitations include the need to address an imbalanced dataset and ECG data variability, as well as the potential for further validation through the evaluation of real-world data and increased image numbers. Classification accuracies of 99%, 99.8%, and 99.89% were achieved in detecting MI using ECG signals with different DL architectures involving CNN, CNN-LSTM, and ensemble method respectively [12].

Ensemble model, Generative Adversarial Network combined with LSTM was proposed [13] with the goal of improving the identification of cardiovascular disorders using ECG signals. On the MIT-BIH and PTB-ECG datasets, this model fared better in accuracy-99.2%, F1-score–98.7%, area under curve (AUC)-98.4% and accuracy-99.4%, F1-score-99.3%, AUC-99.5% respectively. However, the study has limitations as it did not explore alternative ensemble models or different datasets, indicating potential for future research and further validation. The challenge of real-time and accurate categorization of patient-specific ECG signals using compact systems was addressed in [14]. The proposed 1D Self-organized operational neural networks demonstrated enhanced performance compared to CNNs in patient-specific ECG classification. Nevertheless, limitations of the study include dataset bias, lack of comparative analysis, and limited interpretability. Multiple traditional algorithms were tested, and the study identified the three best-performing machine learning algorithms [15] to identify CAD. Data preprocessing techniques, including normalization and optimization using genetic algorithms and particle swarm optimization, were applied to improve algorithm performance. The Z-Alizadeh Sani dataset showed a high accuracy of 93.08% for the suggested method. However, one limitation of the study is its focus on data collected from Iranian patients, which limits the generalizability of the results to other populations. The 1D-CNN Caps Net [16] was employed, which learned relevant representations directly from raw data without manual feature engineering, achieving an accuracy of 99.44%. Despite the absence of a large and diverse dataset, which may impact the generalizability of the results, the suggested model exhibited considerable promise and great potential to aid cardiologists in making a prompt and accurate clinical diagnosis of CAD. In [17] the classification of classes for normal, CAD, MI, and CHF using CNN and Gabor CNN models was strong, topping 98.5%.

The Gabor CNN model showed promise as a technique to help physicians quickly check their classification of CVD diagnosis choices. Nevertheless, a constraint of the study was the use of an imbalanced dataset, necessitating the implementation of weight-balancing techniques. The hybrid deep neural model [18] effectively addressed data imbalance by utilizing focal loss and achieved high sensitivity (97.87%) and specificity (99.29%) in detecting atrial fibrillation using the MIT-BIH atrial fibrillation database. This hybrid model shows potential for real-time atrial fibrillation detection in routine ECG screenings. However, the study had limitations, including limited testing on certain rhythm types and the time-consuming nature of the 10-fold cross-validation process. 1D-CNN with an LSTM model with a precision rate of 98.5% was utilized to categorize 4 different CAD, normal, MI, and CHF classes [19] using ECG signals from physionet.org. without the use of traditional denoising, feature extraction, feature selection methods. The results were interpreted using signals with noise. Using a 95% average accuracy across all classes, the CNN model was utilized to predict 17 distinct forms of cardiac anomalies [20].

Most studies revealed favourable results, yet certain difficulties continue unresolved. Specifically, the suggested system’s categorization performance was ignored among patients. Experts often use a data set containing heart beats drawn from various databases, picking at random part of it for training and the rest for testing. To accurately forecast potential patients in real-world circumstances where heartbeats cannot be utilized as training data, it's important to assess the effectiveness of created algorithms for detecting CVDs amongst patients. In every aspect associated investigations had none a review of the disturbance’s resilience of the setup. In these investigations, the majority of investigators used the data from experiments recorded with no visible disruption, meaning the attributes of ECG patterns are easily apparent. But the signals extracted from real-world environments tend to come with various amounts of disturbances, resulting in the masked appearance traits of the ECG wave patterns. The findings from investigations do not adequately demonstrate the capability of the system to deal with imbalanced data. While others have conducted studies using one-level inconsistent raw data, the extent of data mismatch in real-life situations is varied and unforeseen. So, the research findings are inadequate for illustrating the system's capacity to manage dissimilar input. To match real requirements, the suggested framework needs to be verified with a complex

FOREX Publication
Open Access | Rapid and quality publishing
International Journal of Electrical and Electronics Research (IJEER)
Research Article | Volume 12, Issue 4 | Pages 1301-1323 | e-ISSN: 2347-470X

imbalance collection. Furthermore, while regular ECGs are often much more common than abnormal ECGs in fact, the number of normal ECGs should surpass the quantity of others while assessment.

The DL or hybrid approach presented in many studies, offers several advantages, including improved feature extraction, representation learning, and prediction accuracy. This makes it particularly suitable for complex tasks or datasets where a single deep-learning architecture may not suffice. The approach presented in related studies, interpreted that hybrid models come with increased complexity and computational requirements, which can pose challenges for model optimization and interpretability. From the studies it is also revealed that the challenges related to limited interpretability of deep learning models, the need for large labelled datasets, and real-time implementation difficulties persisted, Further evaluation to validate, larger and more varied datasets are needed to the model's robustness, and there is a need to address an imbalanced dataset and ECG data variability.

This study's objective is to design a hybrid DL architecture capable of reliably classifying ECG signals into several categories of heart disorders. The proposed system encompasses preprocessing the ECG signals by sampling and standard scaling, extracting pertinent features using 1D-CNN, and training the deep learning model developed using appropriately labelled data segments that encompass a range of heart diseases including CAD, MI, CHF, cardiomyopathy and normal. It uses a series of convolutional and pooling layers to extract robust features from the input ECG sequence, negating the need for a separate feature extraction step. As a result, the pre-processed ECG signals are trained and categorized straight away. This suggested effort attempts for better cardio diagnosis along with predicting through finding distinct trends in ECG. By leveraging the capabilities of DL algorithms and incorporating diverse datasets, the proposed approach effectively tackles the challenges associated with CVDs, leading to reliable and precise diagnosis ultimately enhancing patient care and improving treatment outcomes.

3. MATERIALS AND METHODS

The goal of this work is to help forecast different cardiac illnesses using a single ECG-based algorithm including several stages marking with capturing a chaotic ECG signal, natural phenomena contribute to disturbance in indications, given their abundance of info. For the, we make use of a proper pass along with dismiss screen during the preparatory phase, it minimizes interference & generates a cleaner electrical cardiac rhythm. After data division, an individual waveform can be confined providing to identify with variations indicating of some heart ailments. Repmat function can be utilized for expanding the available data to improve the approach adaptability, resulting in an abundance of pattern variability. Combined selection employing categories handles the biased population. This weighed set will be split either sets to be used for testing and training those then goes via the framework to obtain extraction. The framework utilizes 2 distinct composite neural structures to draw its strongly observation traits. This techniques usefulness is examined afterwards using parameters. The outcome is a method which has proven more accurate as well as reliable about identification and forecasting CVD illnesses, perhaps leading to better clinical results.

The presented model follows a two-stage process: data pre-processing and classification. At the initial stage, the ECG data is pre-processed in two levels: sample selection and standard scaling. Next, in the second stage, the two different hybrid models are employed, which classifies them into various classes corresponding to specific CVD conditions. ECG data consists of signals and labels. The signals are stored in a cell array. Labels made of categorical array containing the signals' ground truth. *Figure 2* illustrates the workflow of the proposed method in which ECG data is collected from databases, pre-processed, distributed, trained using proposed model, tested, and validated.

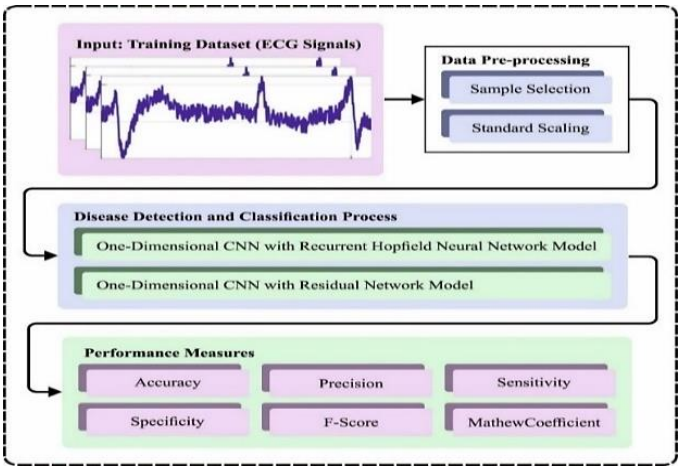

Figure 2. Workflow of the proposed method

3.1. Overview of Database and Pre-processing

PhysioNet.org is used to collect an extensively utilized yet accessible data to examine the success rate of several ECG identification methods. Table 2 lists the databases and its details that were taken into consideration for the investigation of the work. Lead II ECG readings from the specified database are used. To preserve homogeneity, database with low frequency is resampled to 1000 Hz. Preprocessing plays a crucial role in preparing data for DL models. In the context of ECG classification, the following steps are applied:

(a) Structural levels and periods of time, are frequently employed criteria to identify any cardiac event, are two categories of the distinctive properties that the initial ECG signal shows. Lots of sound included in recorded ECGs interfere with appropriate interpretation of these parameters; baseline drift, power line interference, muscle noise, and composite noise are the main ones affected. To eliminate these noticeable noise components in this work, a band pass filter with an appropriate cut-off frequency (0.3 -15Hz) to neglect low and high frequency disturbances and a notch filter (50Hz) are utilized to suppress power line interference. This denoised output seems more uniform as maintains all the pertinent data.

(b) Delineation has significance over vital signs analysis. The design entails dividing a regular ECG into oneself the rhythm of the heart adopting a peak-to-peak data as the starting point.

FOREX Publication
Open Access | Rapid and quality publishing
International Journal of Electrical and Electronics Research (IJEER)
Research Article | Volume 12, Issue 4 | Pages 1301-1323 | e-ISSN: 2347-470X

The structure of the QRS seems critical, presenting to be an index point to serve ci many CVDs recognizing. Each record in the related database is segmented as: Each record's time index is saved and utilized to identify R amplitude (amp) samples, label each identified R-amp, each segment is extracted from the lead II ECG by creating a window about R. Each segment of the ECG signals that were taken out of the database had a window duration of two seconds (2000 samples) resulting in 1,39,795 segments in all. The ECG signal of all classes retrieved, partitioned, and displayed as in *figure 3*.

Table 2. Database details (Physio Net)

Database	Diagnosis	Subjects	Record & Length	Sample Frequency	No. of lead
St. Petersburg INCART 12-lead-arrhythmia database	CAD	7	17 & 0.5Hrs.	257	12
Physikalisch-Technische Bundesanstalt diagnostic ECG Database	MI	148	365 & varies	1000	12
	Normal	52	80 & varies	1000	12
	cardiomyopathy	15	7hcm 8dcm & varies	1000	12
Beth Israel Deaconess Medical Centre Congestive Heart Failure Database	CHF	15	15 & 20Hrs.	250	2
Fantasia Database	Normal	40	40 & 2 Hrs.	250	2

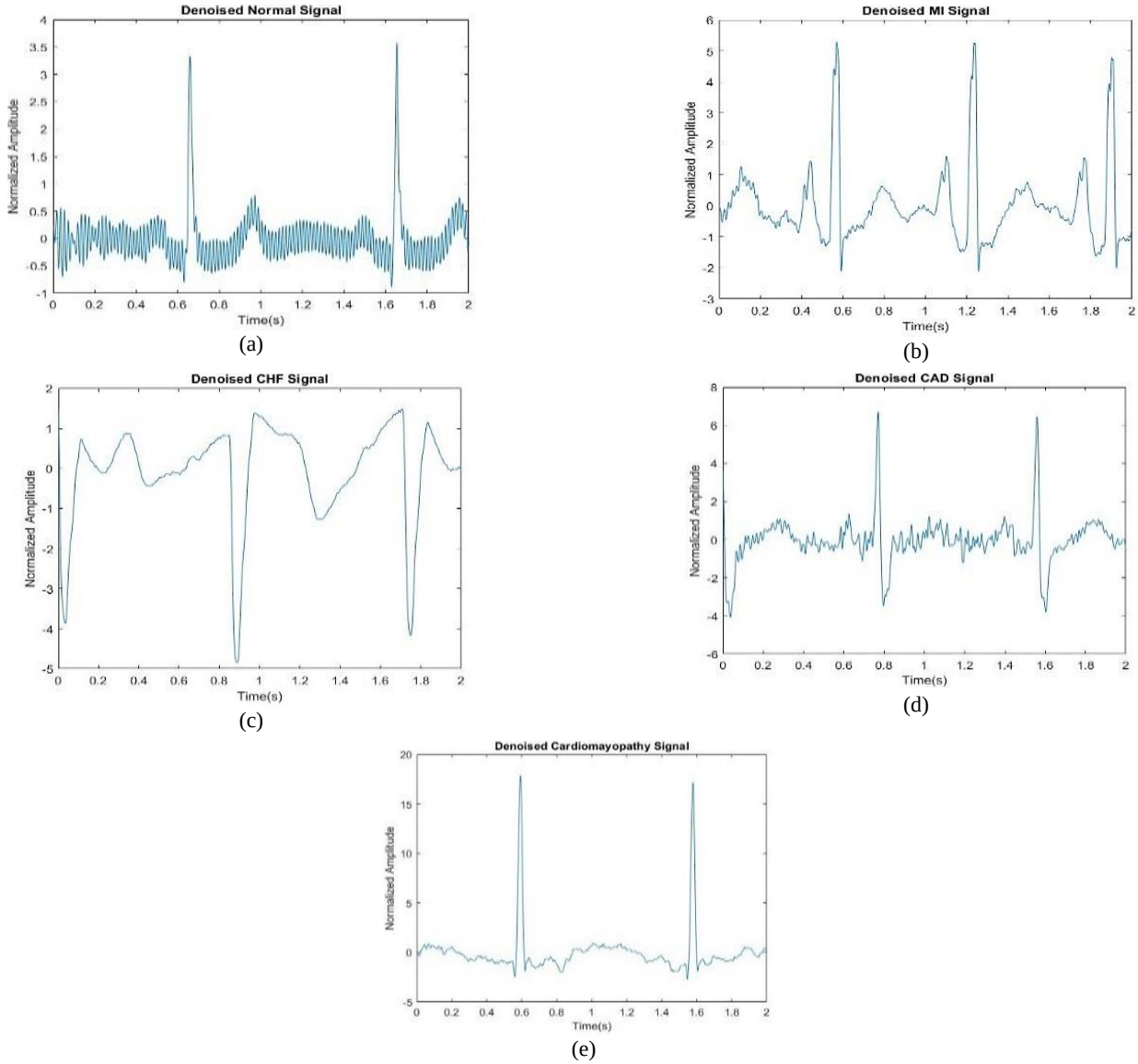

Figure 3. Depiction of CVDs class after removal of noise (a) Normal (b) MI (c) CHF (d) CAD (e) Cardiomyopathy

FOREX Publication
Open Access | Rapid and quality publishing
International Journal of Electrical and Electronics Research (IJEER)
Research Article | Volume 12, Issue 4 | Pages 1301-1323 | e-ISSN: 2347-470X

(c) The input data segments are standardized using the standard deviation (S_D) and mean. The Z-score normalization is used for scaling the input dataset into a uniform format. By using equation (1), the raw data can be modified, Xmean shows the average of variable values, S characterizes the S_D, and Xi indicates the raw value that all the variables continue. Thus, the raw ratio was normalized, with S_D as a unit across samples and the average as 0. By applying these pre-processing steps, a standardized and balanced data can be developed to train the DL model, which helps to accomplish enhanced model performance and stability.

$$Z_{score} = \frac{X_i - X_{mean}}{S} \quad (1)$$

(d) Since the dataset holds a huge number of ECG recordings, it finds it beneficial to elect a subset of data. The segments are taken out of the corresponding database, sorted, labelled, and 7:3 ratios were upheld while selecting the training and testing sets, and an 8:2 ratios was observed when selecting the training and validation sets. Some classes have more training phases than others, while the other class has less. There is a distinction among the dominant and minority classes that must be managed with proper under and over sampling capabilities.

Despite a significant disparity among how many of ECG reads grouped into every kind, the normalized sample remains drastically skewed. Asymmetry may cause distortions with a detrimental effect in how well it performs. Such a mismatch may cause misdiagnosis since the way decisions are made turns in support of the dominant population. For tackling disparities in class, tend to employ resizing means, that incorporate either exceeding or minimizing. Unknown exceedingly along with minimizing have a pair vital resizing. SMOTE [13], the latest resizing concept, serves to deal with uneven class distribution. Inevitably believe these approaches will result in an adequately compatible collection along with an effective representation able managing an array of ECG attributes.

In identifying CVDs applying deep learning, primary characteristics found in ECG segment are often listed here: temporal, morphological, spectral, statistical, non-linear features [45]. The time-domain characteristics of an ECG signal may be utilized for determining RR periods, QRS complex time frame, PR phases, as well QT breaks. The foregoing time-based details may yield facts regarding the occurrence of rhythms, any delays that might occur or anomalies. Physical traits come from the geometry within an ECG pattern. It may comprise the magnitudes as well as regions about a P wave, QRS complex, and T wave, plus the segment ST inclinations. Alteration in them may hint at several kinds of issues with the heart. Harmonic details emerge using the frequency phase in the ECG, which is often obtained using wavelet analysis. It may incorporate both the power and primary harmonics in different ECG groups. Alteration within such harmonic forms may give facts concerning the cyclical & sustained quality that governs the heart's impulses. Probabilistic details encompass cardiac activity gauges like mean, median, variance, skewness, and kurtosis [45]. Such measurements allow for the ECG signal's dispersion and variations. Other attributes include the entropy, fractal dimensions as not parametric, all picked up elements go into a framework that subsequently learns similarities related for different illnesses. The framework's ability to effectively take into consideration an extensive number characteristics & its relationships, which could lead to better reliable along consistent illness determination. For recognizing patterns and variations in ECG, specific traits are derived using separated points of evidence, in emphasis on the QRS structure. The blended structure captures more closely attribute of the QRS in heart rhythms to identify CVDs. Distinct properties encoded within individual ECG are critical in studying CVDs. Every ECG reading linked with an ailment type has different indicators who appear at predictable points. Suggested structure employs advanced computations that precisely distinguish tiny shifts that classify ECG illness condition. Also includes finding the overall quality of signal for each fragment exactly any given point. thereby relying onto the estimated indications, we were able to figure out unique features in each segment. Knowing unique pattern portions is vital to determine ailment kind.

3.2. CNN

CNN may use the convolution process to draw out all relevant characteristics from the input data. Since ECG signals are time-series data, one dimensional convolution applied to analyse them. After receiving the input data, the 1D-CNN generates several label predictions. Broadly speaking, it follows a specific framework made of layers as portrayed in *figure 4*. Convolution, activation, pooling, dropout, flatten, fully connected, and SoftMax are the parts that make up the CNN structure. Each convolution layer comprises of filters, those with smaller sizes might reduce the computation for training the model faster. To get the features from input data according to specifications (filter and step size) and represent those features, locations on the feature map, filters must be trained.

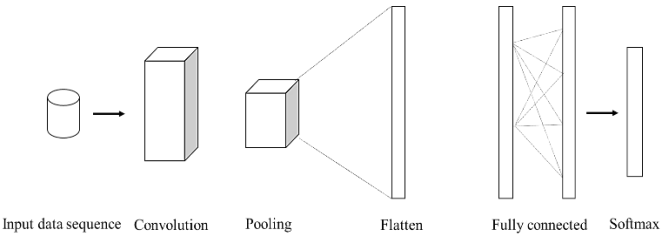

Figure 4. 1D CNN basic structure

The feature map is used as input by the model in the ensuing layers, which generate a new feature map using additional filters. This procedure is carried out in subsequent layers as the retrieved traits get more sophisticated and capable of forecasting. Afterwards, the signals are categorized using the output feature map using the sequential traits that were extracted. An input grid measuring Lw (window length) *Nc (channel count), kernel size Tw * Nc is needed for 1D-CNN, *equation (2)* & *equation (3)* gives the output of each node n and feature map.

$$O_n = f\left(\sum_{i=1}^{T_w} \sum_{j=1}^{N_c} w_i I_{n+i,n+j} + b\right) \quad (2)$$

FOREX Publication
Open Access | Rapid and quality publishing
International Journal of Electrical and Electronics Research (IJEER)
Research Article | Volume 12, Issue 4 | Pages 1301-1323 | e-ISSN: 2347-470X

On – response of each node n, f- activation function, w- weights, b- bias, Tw-is the window of time that each of its levels filters covers.

$$F_m = \frac{filter\ size-(kernel\ size-1)+2\times padding}{stride} \quad (3)$$

In every convolution layer, the activation function is replaced with rectified linear units (ReLU), which lowers computing overhead and fixes vanishing gradient issues. The decision function's selectivity is increased by this structure's use of nonlinear functions. The highest-ranking features were separated out by normalizing each layers each time. Nothing in the pooling and drop out layers would change if used after each convolution layer during training because it lacks any trained parameters but could significantly reduce overfitting. The last is fully connected followed by a single output layer. To support multi-class classification, the activation function utilized in the output layer is SoftMax (4).

$$Q(f_i) = \frac{e^{f_i}}{\sum_{j=1}^{n} e^{f_j}} \quad (4)$$

Q(f)- likelihood that f is connected to i^{th} class, f_i-last layer feature feeds, j- overall quantity of classes.

Every time data points were fed for the structure; the stages of convolution were followed by max pooling to obtain the best attributes for sorting. With the goal to build maps of attributes for the layer that came after, every single phase of convolution was utilized for acquiring traits from the signals that were entered. In order to separate the most compelling features, max pools have been integrated each time that follows the convolution tiers. In an attempt towards enhancing the possible features' interpretation, a dropout component was included. In the course of the model's training stage of the 1D-CNN model using the reverse propagation technique, the gradient values for the weight coefficients on different layers are regularly gathered throughout the training process. We then update the weights using several variations of stochastic gradient descent approaches. For the sake of getting the hybrid version, this structure is altered in a comparable fashion.

3.3. Recurrent Neural Network (RNN)

There are certain repetitions, intervals, or reverse links in the hierarchical arrangement of RNNs. After obtaining the inputs, it generates an output and transmits it again to self. Rolling it out down the temporal axis, it may be thought of as a concatenation of neural networks that use the inputs and outputs of the network at a previous time as input values to recall the history of the data enabling the information to stay in the model for the whole time. As the outcome of the previous cell, the past serves as a transient memory. It can be less effective at making connections between the data, particularly as the gap widens. Extended memory retention is a benefit of the (Long Short-Term Memory) LSTM, which solves the issue of persistent continuous learning and permits the method to employ the stored information for predictions in the future. The fundamental ideas of LSTM functioning are related to gated and cellular states. The cell's condition is the essential element of a component that facilitates movement of data across the whole model. Which data needs to be removed from the current state of the cell is determined applying a sigmoid (σ). It calculates a value representing a cell status for every value between 0 (remove data) and 1(retain data). The subsequent stage determines which pertinent data should be stored in the cell's current level. The parameters that that we'll modify are selected by the sigmoid phase, the state is updated with a series of fresh values generated by an additional layer named (hyperbolic tangent) tanh, the final stage is updating the former state to an alternative cell status. Lastly, output data is determined using the revised cell state version. The outputs of the sigmoid and tanh [12] computations are summed up and used as an additional stage, ensuring that we only obtain the portions that we choose. It employs, the sigmoid one getting a real number as inputs while providing an output that spans 0 to 1, tanh function governs the output data around the values of -1 to1.

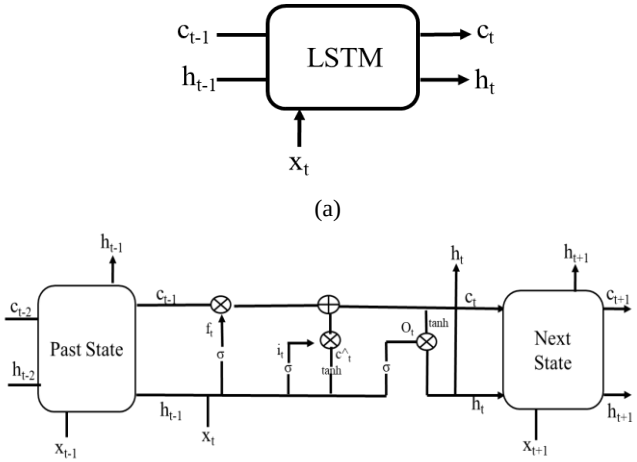

Figure 5. (a) LSTM (b) Repetitive LSTM module [12]

In *figure 5* key terms include forget gate (f_t), input gate (i_t), cell state (C_t), output gate (O_t), and hidden state (h_t), [12] such are updated by distinct biases (b) and factors (w) like in equation (5-9).

$$f_t = \sigma\left(b_f + w_f\,(x_t + h_{t-1})\right) \quad (5)$$

$$i_t = \sigma(b_i + w_i(x_t + h_{t-1})) \quad (6)$$

$$\widehat{c_t} = tanh\left(b_c + w_c(x_t + h_{t-1})\right)$$

$$c_t = i_t\widehat{c_t} + f_t c_{t-1} \quad (7)$$

$$O_t = \sigma\left(b_o + w_o(x_t + h_{t-1})\right) \quad (8)$$

$$h_t = tanh(c_t)\,O_t \quad (9)$$

Bidirectional LSTM (BiLSTM) as in *figure 6*, includes an additional LSTM layer, in which the data that is input travels in both ways, so it has the capacity of deploying data collected from either side, making it an essential forecasting device. It shows the order of inputs runs reversed in the last LSTM layer, after which the results of the two layers are collected in a variety

FOREX Publication
Open Access | Rapid and quality publishing
International Journal of Electrical and Electronics Research (IJEER)
Research Article | Volume 12, Issue 4 | Pages 1301-1323 | e-ISSN: 2347-470X

of methods, like the median, total, multiplying, or linking. To capture the forward and backward information of a data sequence at every step, two LSTMs are joined. This makes recording future features rather than simply the past easy. As a result, the input sequence is trained using two LSTMs: one employs the standard LSTM, while the other adopts a reversed duplicate of the input sequence. Next, the forward and backward hidden state outputs will be concatenated to generate the final vector. This can aid the network in comprehending the issue more rapidly and completely.

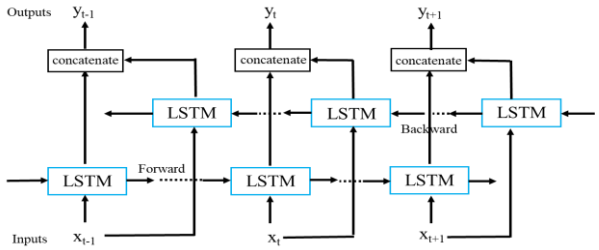

Figure 6. BiLSTM module [21]

A family of RNNs with uniformly sized connections across layers was presented by Hopfield in 1982 and has memory function along with it. All units in this network get their output as input, with the exception of the unit itself. Keeping track of a given collection of patterns and retrieving the related match when the network is provided an approximation of the pattern is the use of memory. Through the manipulation of node values, a pattern is inserted into the network. Next, updated pattern is read out by running the network on a particular input by hebbian learning [22]. *Figure 7* represents the infrastructure of Hopfield Neural Network (HNN).

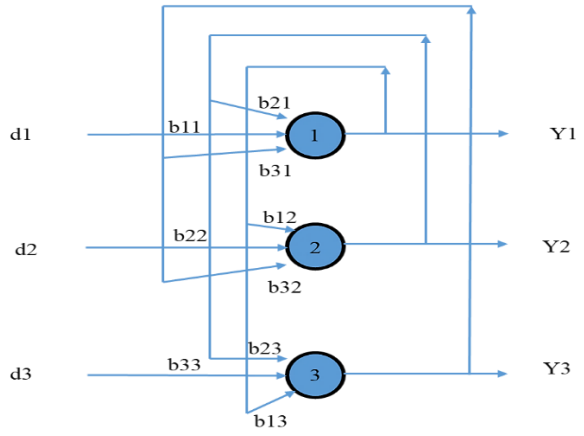

Figure 7. Architecture of HNN with 3 nodes

The procedure is provided below to help you save and retrieve patterns in a HNN [22]. An input and output are the *n* number of neurons in the single layer of the network, N set of fully connected neurons. Taking into consideration a network with N units, each of which has an output function with a bipolar threshold. Let dm, *m*=1,2….M be the data need to be stored, each of it is composed of dmi= [+1, -1], *i*=1,2…N.

a. Set the HNN response to its initial value using the supplied stimuli 'd', *equation (10).*

$$Y_i(0) = d_i \tag{10}$$

i=1,2…N, Yi(0)-response of unit i at time t=0.

b. Put the connecting weights in place, *equation (11).*

$$b_{ij} = \sum_{i=1}^{M} d_{mi} d_{mj}, i \neq j \tag{11}$$

$$b_{ij} = 0, \mathrm{i} = \mathrm{j}, \mathrm{m} \leq \mathrm{i}, \mathrm{j} \leq \mathrm{N}$$

c. Repeat to get final HNN response, *equation (12).*

$$Y_i\,(t+1) = sgn \sum_{j=1}^{N} b_{ij} y_j(t) \tag{12}$$

The learning parameters are utilized to construct the weight matrix, which is updated using the *equation (13),* for each bij, weight from i to j neuron, y (0) =S, Si – typical vector.

$$b_{ij} = \sum_{i=1}^{n} S_i (S_i)^T \tag{13}$$

The following set of dimensionless non-linear ordinary differential equations defined the HNN with n neurons as in *equation (14).*

$$X = -x + B\tanh(x) + I \tag{14}$$

$$B = \begin{bmatrix} b_{11} & b_{12} & \dots & b_{1j} & \dots & b_{1n} \\ b_{21} & b_{22} & \dots & b_{2j} & \dots & b_{2n} \\ \vdots & \vdots & \ddots & \vdots & \vdots & \vdots \\ b_{i1} & b_{i2} & \dots & b_{ij} & \dots & b_{in} \\ \vdots & \vdots & \vdots & \vdots & \ddots & \vdots \\ b_{n1} & b_{n2} & \dots & b_{nj} & \dots & b_{nn} \end{bmatrix} x = \begin{bmatrix} x_1 \\ x_2 \\ \vdots \\ x_i \\ \vdots \\ x_n \end{bmatrix} I = \begin{bmatrix} I_1 \\ I_2 \\ \vdots \\ I_i \\ \vdots \\ I_n \end{bmatrix} \tag{15}$$

In *equation (15),* Ii shows i^{th} neuron external stimulate current, and xi represents the i^{th} neuron membrane voltage. B signifies the synaptic weight matrix, *bij* indicates the synaptic weight between j^{th} and i^{th} neurons.

3.4. Residual Neural Network (ResNet)

ResNet, an acronym for residual network, describes the remaining building components that comprise the network's design. For the CNN model, every input layer is predicated on the previous layer's output, thus, if a model has too many layers, it might suffer from the problem of collapsing because of the gradient computation. Therefore, a residual structure was introduced with the 'shortcut/skip' structures [23]. Training of deep networks with large number of layers is possible, as it is built on a deep residual learning architecture. To guarantee that increasing layers does not result in a loss of training performance, the network is simply instructed to construct an optimum mapping when these residuals are near to zero. It is a collection of residual blocks in which the network may learn more accurate representations of the input which enable the retention of information from previous levels. *Figure 8,* provides a graphic representation of module.

FOREX Publication
Open Access | Rapid and quality publishing
International Journal of Electrical and Electronics Research (IJEER)
Research Article | Volume 12, Issue 4 | Pages 1301-1323 | e-ISSN: 2347-470X

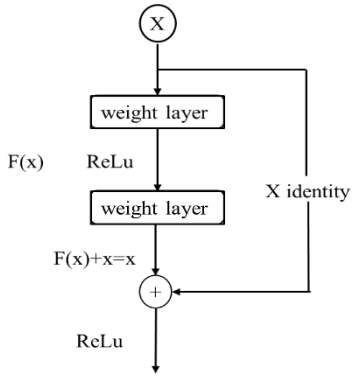

Figure 8. Basic residual block [23]

Compared to the initial mappings, maximizing residual mappings is simpler the middle layer output has been added to the initial layer. The residual model instead learned the difference between a congruent mapping and an ideal solution like *equation (16)* as opposed to learning input and output mapping.

$$F(x) = H(x) - x \tag{16}$$

where H(x) shows the optimum solution and x denotes the congruent mapping. And hence, H(x) = F(x) + x would be the new formulation. The input from the preceding layer is the source of each layer's processing in CNN. ResNet considers both the output of the preceding layer and the network structure that existed before the layer's output. Consequently, enough data can be extracted from the input characteristics. Skipping more than two levels, it carries out identity mapping. These networks are spared the extensive convolution layers that cause performance reduction in simple networks.

4. ECG SIGNAL CLASSIFICATION

During the ECG data classification process, the altered data segments is fed into the DL model, a series of 2000 data points is collected for feeding into the model of a neural network. In this study, 1D CNN with ResNet and RHNN are used for the categorization of different types of CVDs. In addition to having a preset structure that may be changed based on the application, CNN can produce features without human input. Using the suggested method to identify cardiac dysfunction will include the following experimental phases.

1. Preparing Data

Importation of data- To do a classification that involves multiple classes ranging from L1 to L5, load the data points and the associated labels.

Cleaning- By addressing the absence of values and outliers and restoring the values, you are able to clean up the collected information.

Modification of specific information- Given the predominantly laid out nature of the dataset, this would entail constructing duplicates through potential applications of random over sampler and under sampler.

2. Structure Construction

Initial model- With a considerable amount of architectural change, use the 1DCNN architecture to deduce related attributes from data that is ordered.

Improvisation- The original CNN framework is merged with the RHNN and ResNet.

3. Learning

Select an appropriate loss function, specific cross entropy, for the use of multiclass.

Train the illustrated model with optimizers such as Adam or RMS Prop.

4. Assessment

To track how well the predicted outcome performs during learning, divide the available data into sets to be used for validation and training.

4.1. 1D CNN-RHNN

Short-term variation aspects of ECG readings may be obtained through CNN when used, the data points begin by being transformed into a folded vector, after which they undergo computational processing in the hidden layers via the activation function, and the output forecasts group chances. One dimension is slide by the kernel in a 1DCNN to fit the dimensions of the ECG signal. As filters are employed across a CNN's sections, characteristics are learnt about the ECG. Both a CNN and RNN make up the put forward type. The RNN was trained to handle the task of classifying heartbeats by using the extracted sequence characteristics from the raw time series ECG data as input. First, the CNN layer was used to generate the model's layer by layer. We also experimented with normalization, max-pooling, and thick layers to enhance the model's performance. Dropout layers tried at several points in the model with values (0.0 to 0.5) to preserve regularization. Until the ideal number of layers and ideal hyper parameter are attained, the procedure is repeated. Prior to deciding on the final layer, several hybrid structural arrangements were tried.

The 1D CNN-RHNN model as in *figure 9* is a hybrid DL model that integrates the benefits of 1-D CNN with the RHNN model for ECG classification. The 1-D CNN is designed for capturing patterns within the ECG signal. It includes non-linear activation function, pooling, and different convolutional layers. The convolutional layer performs feature extraction by sliding smaller filters across the ECG signals, which capture related patterns. The pooling layer down sample the extracted feature, decreasing the dimensionality while preserving relevant data. At the same time, the RHNN is accountable to capture long-term temporal dependency in the ECG signal and enables the network for storing and recalling patterns over time. The output from the CNN element is fed into the RHNN that exploits recurrent connections for processing the temporal data and further refining the representation.

FOREX Publication
Open Access | Rapid and quality publishing
International Journal of Electrical and Electronics Research (IJEER)
Research Article | Volume 12, Issue 4 | Pages 1301-1323 | e-ISSN: 2347-470X

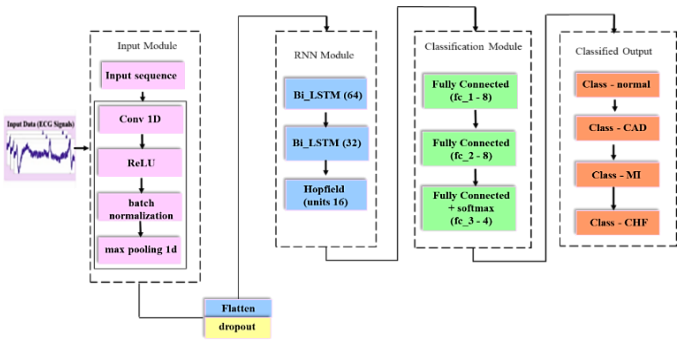

Figure 9. Schematic block of 1D CNN-RHNN model

A total of five levels of CNN, containing 3,6 points, make up the topology. Every value of 20,10,5, 5,10 the kernel appeared set. It has a single stride and proper padding throughout. To sort out suitable types, an extra layer of BiLSTM with 64 and 32 portions each together, hopfield sections of 16 is integrated with the CNN in the very last phase. Next, to flatten the data to the size required by the thick layer of data, the global value pooling was done followed by thick with drop out layer that simulates after the CNN. Lastly, softmax is applied for categorization. Table 3 gives specifics of all layers along with its traits. To decrease the characteristic size, this experiment deployed a 1D CNN component to retrieve features. RHNN was subsequently took advantage towards forecast.

Table 3. Specifics of 1D CNN-RHNN

Kind of Layer	Resultant (Final) Form	Dimension (kernel, stride)
Sequence input with 1d	2000×1	-
Conv1d_1	1981×3	20,1
relu_1	1981×3	-
batchnorm_1	1981×3	-
maxpoolind1d_1	990×3	2
Conv1d_2	981×6	10,1
relu_2	981×6	-
batchnorm_2	981×6	-
maxpoolind1d_2	490×6	2
Conv1d_3	486×6	5,1
relu_3	486×6	-
batchnorm_3	486×6	-
maxpoolind1d_3	243×6	2
Conv1d_4	239×6	5,1
relu_4	239×6	-
batchnorm_4	239×6	-
maxpoolind1d_4	119×6	2
Conv1d_5	110×6	10,1
relu_5	110×6	-
batchnorm_5	110×6	-
maxpoolind1d_5	55×6	2
bilstm_1-bilstm_2-hopfield_1	64-32-16	-
dense (fc_1) with dropout	8	-
dense (fc_2) with dropout	8	-
dense (fc_3)+softmax	4	-

4.2. 1-D CNN-ResNet

1D-CNN was introduced to categorize many features. it reduces the feature and maps its internal features from the 1D data stream and uses fixed-length data and the feature was positioned at every point along the segment. The structure of the 1DCNN-ResNet model is depicted in *figure 10*.

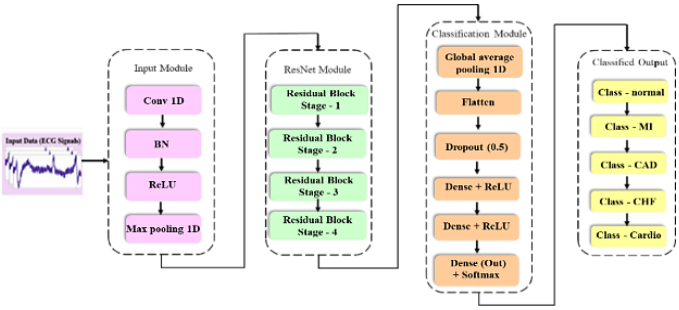

Figure 10. Schematic block of 1D CNN-ResNet model

An input, a residual, and a classification module make up the suggested model architecture. 1D convolution layer (conv1D, filters (F)-16, kernel (K)-10, sride (S)-1), batch normalization layer (BN), rectified linear unit activation layer (ReLU), and a max pooling layer (S-2) make up the input module. In addition, extensive features have been extracted using residual blocks. The residual module can be divided into two categories: (a) residual_1 (convolution) includes 3 conv1d (K-1, 3, 1, S-1), 3 batchnorm1d, and 3 (ReLU) activation layers. To correspond to the dimensions and bypass links, 1 conv1d (K-1, S-2), 1 batchnorm1d, 1 ReLU layer are use on the other side. (b) residual_2 (identity) includes 3 conv1d (K-1, 3, 1, S-1), 3 batchnorm1d, and 3 (ReLU) activation layers. The last module in the structure is a classification model. First, 1d global average pooling receives the residual module's response, which is then summarized and fed to classification model. Here, the feature map matrix derived from the residual model is flattened into a single column and then submitted to the network. To stop the ResNet from being over-fitted, a dropout layer was next added. Then, the 2 thick layer was activated by ReLU. To determine the probability distribution and assign a class from the given list of targets, the softmax function is used at the last thick layer to achieve high scores for specified testing or training samples. This process ensures effective classification and accurate representation of the model's output. The residual part like *figure 11* has a dissimilar fusion of layers as follows: convolutional and identity blocks. Each section of the claimed structure is laid out further in the *table 4.*

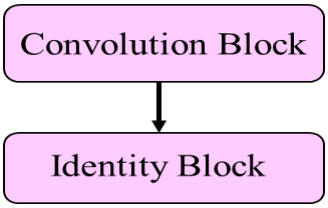

(a)

FOREX Publication
Open Access | Rapid and quality publishing
International Journal of Electrical and Electronics Research (IJEER)
Research Article | Volume 12, Issue 4 | Pages 1301-1323 | e-ISSN: 2347-470X

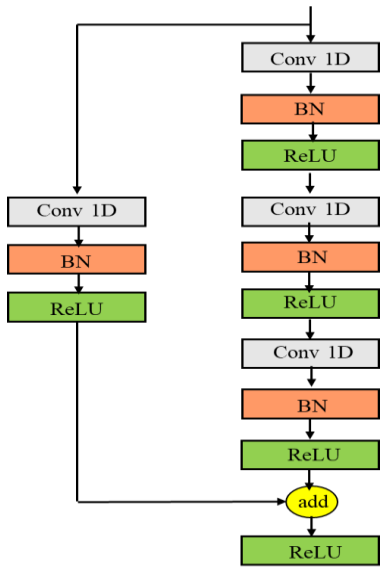

(b)

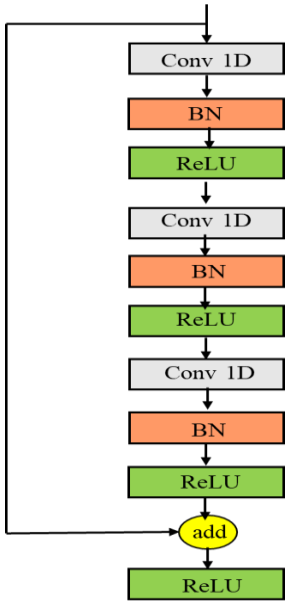

(c)

Figure 11. ResNet module architecture [24] (a) Residual block (each stage) (b) Convolution block (c) Identity block

Table 4. Specifics of the 1D CNN-ResNet structure (a) Input module (b) Residual module (c) Classification module

Table 4(a)

Input module	
Kind of Layer	Parameter
conv1d	224016
batch-norm	64
relu activation	-
maxpoolind1d	-

Table 4(b)

Residual module		**Residual module (continued)**	
Kind of layer	**Parameter**	**Kind of layer**	**Parameter**
conv1d, 16	272	conv1d, 256	16640
conv1d, 16	784	conv1d, 256	16640
conv1d, 64	1088	add	-
conv1d, 64	1088	activation	-
Add	-	conv1d, 64	16448
Activation	-	conv1d, 64	12352
conv1d, 16	1040	conv1d, 256	16640
conv1d, 16	784	conv1d, 256	65792
conv1d, 64	1088	add	-
conv1d, 64	4160	activation	-
Add	-	conv1d, 64	16448
Activation	-	conv1d, 64	12352
conv1d, 16	1040	conv1d, 256	16640
conv1d, 16	784	conv1d, 256	65792
conv1d, 64	1088	add	-
conv1d, 64	4160	activation	-
Add	-	conv1d, 64	16448
Activation	-	conv1d, 64	12352
conv1d, 32	6176	conv1d, 256	16640
conv1d, 32	3104	conv1d, 256	65792
conv1d, 32	1056	add	-
conv1d, 32	3104	activation	-
conv1d, 128	4224	conv1d, 64	16448
conv1d, 128	4224	conv1d, 64	12352
Add	-	conv1d, 256	16640
Activation	-	conv1d, 256	65792
conv1d, 32	4128	add	-
conv1d, 32	3104	activation	-
conv1d, 128	4224	conv1d, 128	98432
conv1d, 128	16512	conv1d, 128	49280
Add	-	conv1d, 128	16512
Activation	-	conv1d, 128	49280
conv1d, 32	4128	conv1d, 512	66048
conv1d, 32	3104	conv1d, 512	66048
conv1d, 128	4224	add	-
conv1d, 128	16512	activation	-
Add	-	conv1d, 128	65664
Activation	-	conv1d, 128	49280
conv1d, 64	24640	conv1d, 512	66048
conv1d, 64	12352	conv1d, 512	262656
conv1d, 64	4160	add	-
conv1d, 64	12352	activation	-

Table 4(c)

Classification module	
Kind of Layer	**Parameter**
global_average_pooling1d	-
flatten	-
Dense (output)	2565

The ECG sequence was fed as input to the 1D convolution layer with adaptive learning of convolutional kernel. Then, we utilized a ReLU activation layer, which enables positive output while thresholding the residual output to zero and further if required batch normalization can be used to normalize the input, input block was followed by pooling layer. The residual part input was taken to be the output of the input. The residual learning part was broken down into four phases, each of which included an identity block and a convolutional block. The recommended approach is illustrated as follows: The input data sequence, often referred to as the input tensor, is fed into the model's first convolutional layer. This layer extracts early

FOREX Publication
Open Access | Rapid and quality publishing
International Journal of Electrical and Electronics Research (IJEER)
Research Article | Volume 12, Issue 4 | Pages 1301-1323 | e-ISSN: 2347-470X

characteristics from the input to prepare it for additional processing *eq. (17)*.

$$S_{conv1} = \sigma\big(N(w_{conv1} * I + b_{conv1})\big) \quad (17)$$

σ –relu function, N- batch normalization, wconv1-weights, bconv1-bias, I- sequence input Subsequently, residual block as it is made up of several layers with convolution and identity blocks handles the response from input block. The shortcut route link, the main characteristic of this block, enables activations to bypass one or more layers, hence assisting in resolving the vanishing gradient problem. Each convolution inside the block is identical to that found in *eq. (18)*, *i*-specific layer. Should one exist, a shortcut link is indicated by *eq. (19)*.

$$S_{res} = \sigma\big(N(w_{convi} * I + b_{convi})\big) \quad (18)$$

$$S_{shortcut} = W_{shortcut} * S_{previous} + b_{shortcut} \quad (19)$$

when paired with the main path *eq. (20)*

$$S_{out} = \sigma(S_{res} + S_{shortcut}) \quad (20)$$

This is how the relu is represented as in *eq. (21)*

$$X(z) = \max(0, z) \quad (21)$$

The activation function is then used to pool the traits and summarize them as *eq. (22)*

$$Y_{pool} = [Y_{avg}, Y_{max}] \quad (22)$$

The thick layer produces the final forecasts *eq. (23)*

$$Y_{dense1} = \sigma\big(w_{d1} y_{pool} + b_{d1}\big) \quad (23)$$

The last layer applies softmax *eq. (24)* which receives feature feeds to facilitate several-label categorization.

$$Y_{out} = \text{sofmax}(w_{d2} y_{dense1} + b_{d2}) \quad (24)$$

wd1, wd2, bd1, bd2 – weights and bias of dense layer.

As stated in *eq. (25)*, the loss is utilized to evaluate the difference between the target class probability c(f) and the anticipated output probability q(f).

$$loss = E\big(c(f), q(f)\big) = -\sum_{m=1}^{k} c_m(f) log q_m(f) \quad (25)$$

The design is made quicker and more reliable by using the batch normalization 1d phases, while the conv1d tiers serve to extract properties. Average Pooling serves to pool the traits that the remaining blocks have retrieved. The combined data are subsequently assembled and given to the final section, to provide predictions.

5. EVALUATION METRICS

Regularly used metrics to assess categorization performance include accuracy ($accu_y$), precision ($prec_n$), specificity ($spec_y$), Mathew correlation coefficient (MCC), recall ($sens_y$), and F-score. These metrics are found using *equation (26) to (31)*, the categorization performance is interpreted using confusion matrix which is a table that compares the predicted class labels to the genuine class labels to summarize the performance of a classification model. It shows how many true positives (TP), true negatives (TN), false positives (FP), and false negatives (FN) were predicted by the model. All the metrics for each class is evaluated and the average of the same is also computed.

$$\text{Accuracy}_{class0} = \frac{(TP_{class0}+TN_{class0})}{(TP_{class0}+TN_{class0}+FP_{class0}+FN_{class0})} \quad (26)$$

$$\text{Precision}_{class0} = \frac{TP_{class0}}{(TP_{class0}+FP_{class0})} \quad (27)$$

$$\text{Recall}_{class0} = \frac{TP_{class0}}{TP_{class0}+FN_{class0}} \quad (28)$$

$$Specificity_{class0} = \frac{TN_{class0}}{TN_{class0}+FP_{class0}} \quad (29)$$

$$F - score = \frac{2*recall*precision}{recall+precision} \quad (30)$$

$$\text{MCC}_{class0} = \frac{TP_{class0}*TN_{class0}-FP_{class0}*FN_{class0}}{\sqrt{(TN_{class0}+FN_{class0})(TP_{class0}+FP_{class0})(TN_{class0}+FP_{class0})(FN_{class0}+TP_{class0})}} \quad (31)$$

6. EXPERIMENTAL VALIDATION

The proposed hybrid model is interpreted considering 4 and 5 classes. A complete set of 1,39,795 ECG parts, including 78000 regular, 17325 MI, 29250 CHF, 14450 CAD, and 770 cardiomyopathy sections, are obtained during the study. The databases employed include Physikalisch-Technische Bundesanstalt diagnostic ECG Database (PTBDB), Beth Israel Deaconess Medical Centre Congestive Heart Failure Database (BIDMC-CHF), Fantasia and St Petersburg Institute of Cardio logical Technics 12-lead Arrhythmia Database (INCARTDB). In this section, the ECG classification results of the presented method are examined on the ECG dataset comprising 40000 segments chosen randomly and include normal, CHF, CAD, MI class. Each class holds a set of 10000 segments, for the classification. The trial is run on a data set that is balanced. Below is the order of the data elements in 4 types sorting groups: Data-40000, Train-28000, Test-12000. 5 types sorting groups include Data-8770, Train- 6139, Test-2631 segments respectively. We identified the best possible parameters for the models after extensive trials. Initially, an CNN framework was created with these criteria: a batch of 10, 60 epochs, rate of learning 0.001, with Adam optimizer [25]. As the loss is calculated, weight balancing modifies the weight of the training data to assist maintain data balance. It was trained using the attained signals and the most promising features were linked. The RMS prop required more calculation time than the Adam optimizer while compiling, but there was no difference in the correctness, resulting in choosing the later one for compiling the models. The experimental analysis of the method involves the flow as in *figure 12*, implemented using python 3.10.10 with keras library (tensor flow) and experimented on graphics processing unit. Suitable fractioned verified the data tagged in the segment.

FOREX Publication
Open Access | Rapid and quality publishing
International Journal of Electrical and Electronics Research (IJEER)
Research Article | Volume 12, Issue 4 | Pages 1301-1323 | e-ISSN: 2347-470X

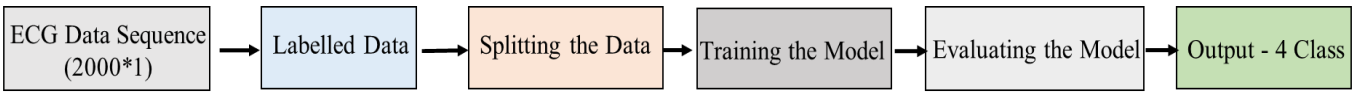

Figure 12. Flow of model analysis

6.1. Analysis of 1D CNN-RHNN to Categorize Four Classes

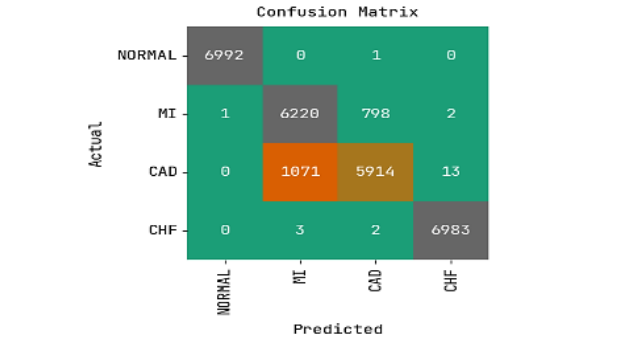

(a)

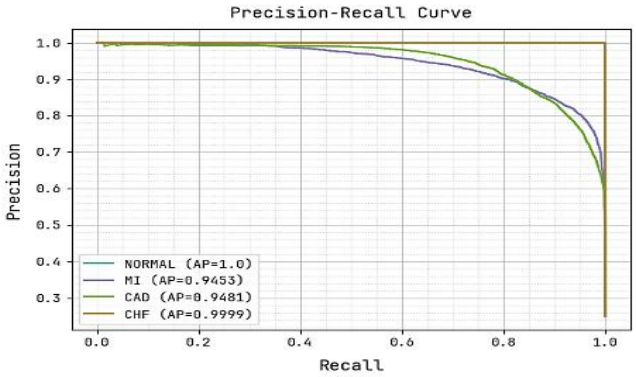

(b)

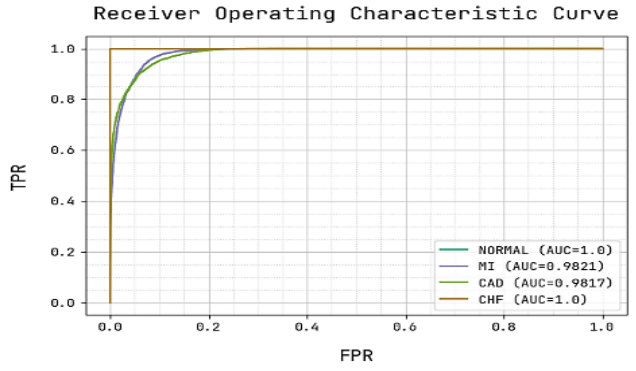

(c)

Figure 13. Training set analysis on 1D CNN-RHNN (a) Confusion matrix (b) PR-curve (c) ROC-curve

Figure 13, demonstrates the classifier outcomes of the 1D CNN-RHNN technique on train set. *Figure 13a* illustrate the confusion matrix, it identified 4 class labels accurately. *Figure 13b*, reveals the precision recall study of the model, it highlighted that it achieved the highest PR performance among the 4 classes. Finally, *figure 13c* demonstrate the ROC study of the model for train dataset. According to the graph, the approach produces useful results with higher ROC values.

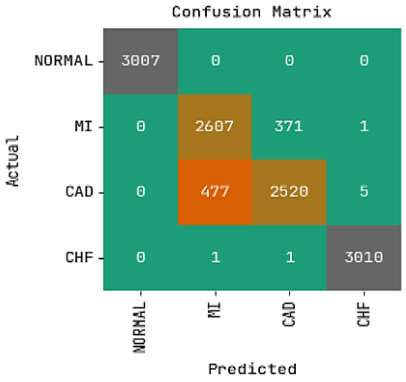

(a)

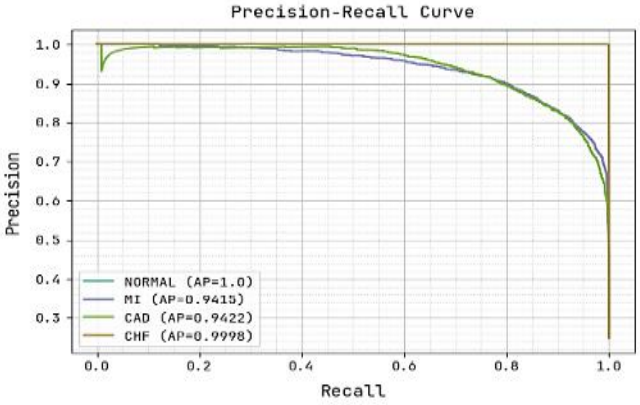

(b)

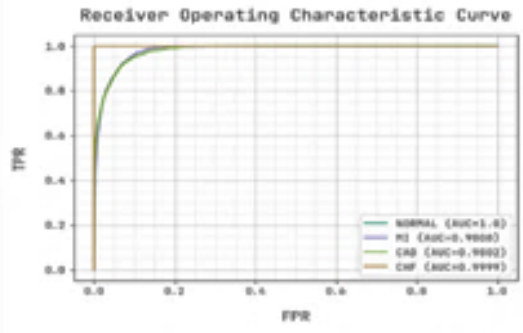

(c)

Figure 14. Testing set analysis on 1D CNN-RHNN (a) Confusion matrix (b) PR-curve (c) ROC-curve

Figure 14a illustrate the confusion matrix granted by the 1D CNN-RHNN method on test dataset, it pointed out that the approach has classified 4 class labels accurately. *Figure 14b*, reveals the precision recall study of the model, Finally, *figure 14c* demonstrate the ROC study of the model for test dataset. In

FOREX Publication
Open Access | Rapid and quality publishing
International Journal of Electrical and Electronics Research (IJEER)
Research Article | Volume 12, Issue 4 | Pages 1301-1323 | e-ISSN: 2347-470X

table 5, the ECG classification results of the same are examined under distinct classes. The results specify that it identifies classes properly. For example, on training set, the 1DCNN-RHNN method attains average $accu_y$ of 96.62%, $prec_n$ of 93.28%, $sens_y$ of 93.25%, $spec_y$ of 97.75%, Fscore of 93.25%, and MCC of 91.01%. At the same time, on testing set, the 1DCNN-RHNN method attains average $accu_y$ of 96.43%, $prec_n$ of 92.86%, $sens_y$ of 92.84%, $spec_y$ of 97.62%, Fscore of 92.84%, and MCC of 90.48%.

Table 5. Classifier outcome of 1D CNN-RHNN approach with distinct measures in percentage

1D CNN-RHNN (Training Set)						
Class	**Accuracy**	**Precision**	**Sensitivity**	**Specificity**	**F-Score**	**MCC**
NORMAL	99.89	99.42	99.64	99.12	99.92	99.69
MI	93.30	85.28	88.59	94.88	86.90	82.43
CAD	93.27	88.07	84.51	96.19	86.25	81.83
CHF	99.93	99.79	99.93	99.93	99.86	99.81
Average	96.62	93.28	93.25	97.75	93.25	91.01
1DCNN-RHNN (Testing Set)						
NORMAL	99.98	99.89	99.98	99.98	99.98	99.98
MI	92.92	84.51	87.51	94.70	85.98	81.27
CAD	92.88	87.14	83.94	95.87	85.51	80.82
CHF	99.93	99.80	99.93	99.93	99.87	99.82
Average	96.43	92.86	92.84	97.62	92.84	90.48

The accuracy of the 1D CNN-RHNN method in the training and validation of the test database is examined in *figure 15a*. According to the outcome, it achieves higher accuracy values with 100 number of epochs. Additionally, it demonstrated effective learning at rate 0.00001 on the test database by showing an increasing validation accuracy over training accuracy. *Figure 15b*, presents the loss analysis of the approach during both training and validation phases on the test database.

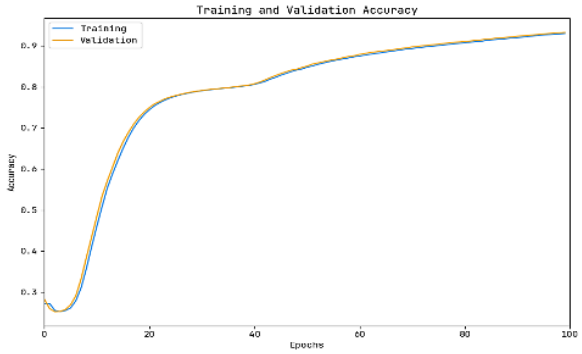

(a)

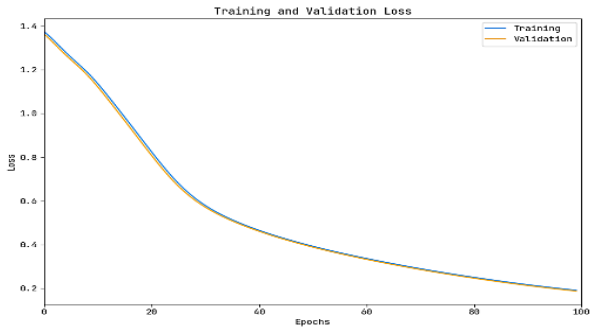

(b)

Figure 15. (a) Accuracy and (b) loss versus number of epochs plot of the 1D CNN-RHNN approach

6.2. Analysis of 1D CNN-ResNet to Categorize Four Classes

In *figure 16a*, the confusion matrix for training dataset is shown, indicating accurate identification and classification of all 4 class labels. *Figure 16b*, display the precision recall study of the method, revealing the highest precision recall performance across the classes. *Figure 16c*, present the ROC analysis of the method, demonstrating valuable results with higher ROC values for the classes with 4 labels.

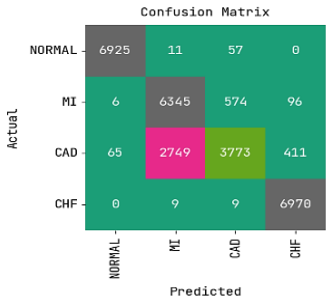

(a)

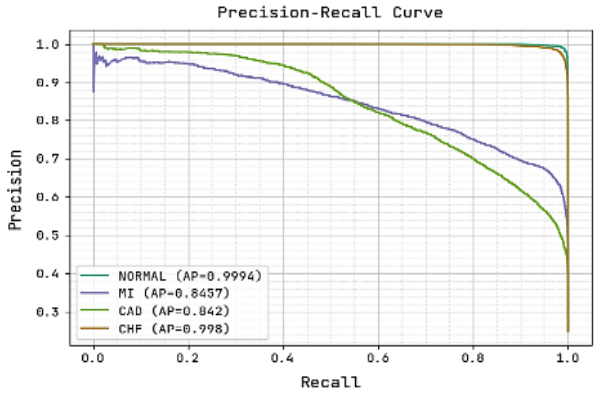

(b)

FOREX Publication
Open Access | Rapid and quality publishing
International Journal of Electrical and Electronics Research (IJEER)
Research Article | Volume 12, Issue 4 | Pages 1301-1323 | e-ISSN: 2347-470X

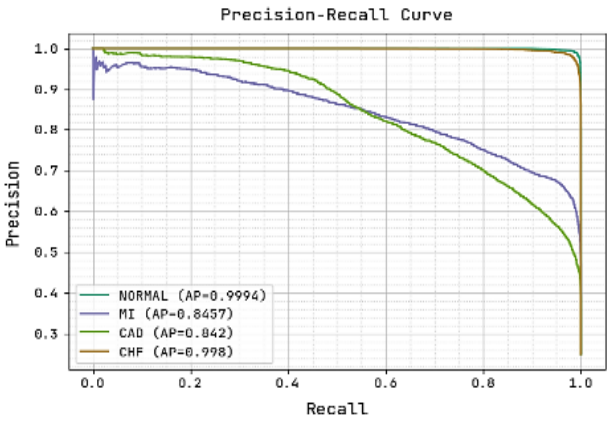

(c)

Figure 16. Training set analysis on 1D CNN-ResNet (a) Confusion matrix (b) PR-curve (c) ROC-curve

Figure 17, illustrates the classifier outcomes of the 1D CNN-ResNet method on the test dataset. In *figure 17a*, the confusion matrix for test dataset is shown, indicating accurate identification. *Figure 17b*, display the precision recall study of the method, revealing the highest precision recall performance. *Figure 17c*, present the ROC analysis of the model, demonstrating valuable results with higher ROC values. In *Table 6*, the ECG classification results are investigated under various classes. The findings show that the 1D CNN-ResNet approach correctly distinguishes between four classes. For instance, on training set the 1DCNN-ResNet technique attains average $accu_y$ of 92.88%, $prec_n$ of 86.83%, $sens_y$ of 85.76%, $spec_y$ of 95.25%, Fscore of 85.04%, and MCC of 81.43%. At the same time, on testing set, the 1DCNN-ResNet technique acquires average $accu_y$ of 92.84%, $prec_n$ of 86.75%, $sens_y$ of 85.68%, $spec_y$ of 95.24%, Fscore of 84.91%, and MCC of 81.32%.

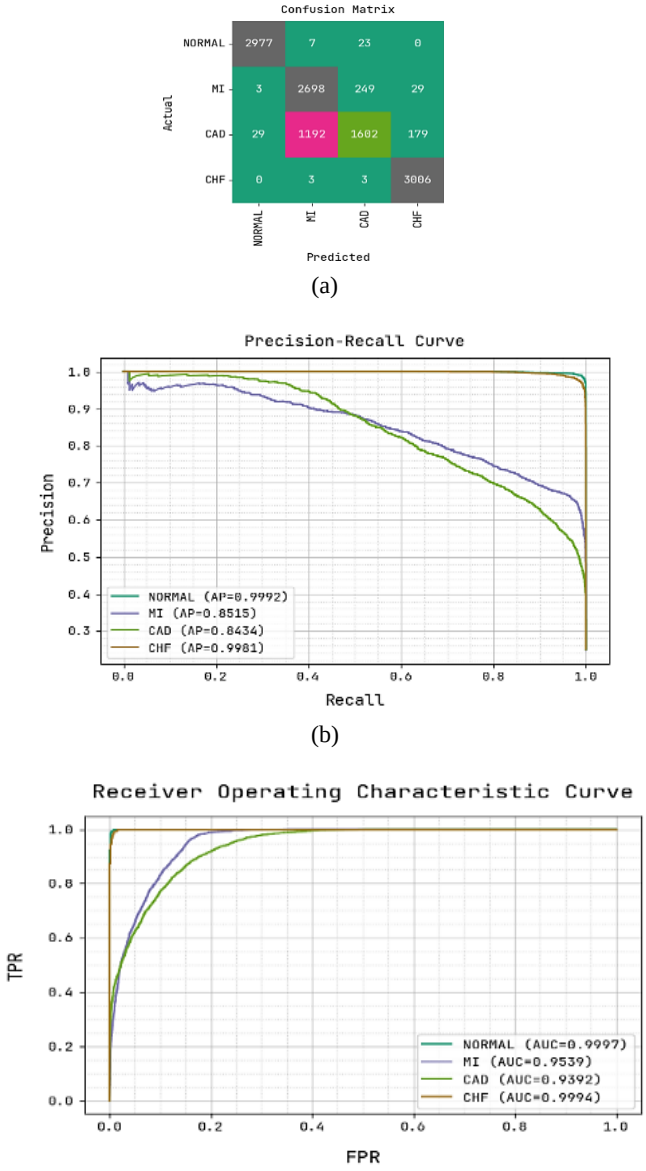

(a)

(b)

(c)

Figure 17. Testing set analysis on 1D CNN-ResNet (a) Confusion matrix (b) PR-curve (c) ROC-curve

Table 6. Classifier outcome of 1D CNN-ResNet approach with distinct measures in percentage

1D CNN-ResNet (Training Set)						
Class	**Accuracy**	**Precision**	**Sensitivity**	**Specificity**	**F-Score**	**MCC**
NORMAL	99.50	98.99	99.03	99.66	99.01	98.68
MI	87.70	69.62	90.37	86.80	78.65	71.39
CAD	86.20	85.50	53.92	96.95	66.13	60.44
CHF	98.12	93.22	99.74	97.59	96.37	95.21
Average	**92.88**	**86.83**	**85.76**	**95.25**	**85.04**	**81.43**
1DCNN-ResNet (Testing Set)						
NORMAL	99.48	98.94	99.00	99.64	98.97	98.62
MI	87.64	69.18	90.57	86.68	78.44	71.24
CAD	86.04	85.35	53.36	96.94	65.67	59.98
CHF	98.22	93.53	99.80	97.69	96.56	95.45
Average	**92.84**	**86.75**	**85.68**	**95.24**	**84.91**	**81.32**

FOREX Publication
Open Access | Rapid and quality publishing
International Journal of Electrical and Electronics Research (IJEER)
Research Article | Volume 12, Issue 4 | Pages 1301-1323 | e-ISSN: 2347-470X

Figure 18a, investigates the 1D CNN-ResNet method's precision while being trained and validated on the ECG database. It indicates that higher epochs provide the approach higher accuracy values. Furthermore, this approach effectively learns from the database with the learning rate of 0.0001 as evidenced by the increased validation accuracy compared to training accuracy. The loss analysis of the model is also shown in *figure 18b*, which revealed that the approach achieved closer training and validation loss values. During training and validation, the model acquired the data over the course of 100 epochs, batch size-32 demonstrating their resilience.

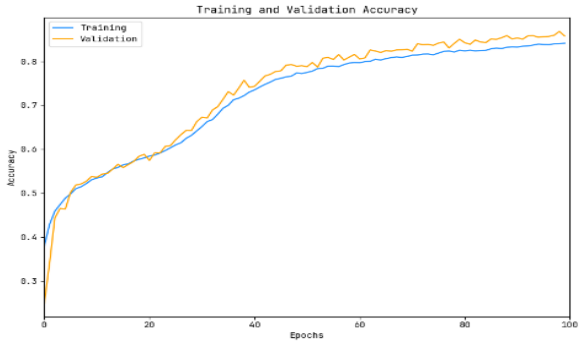

(a)

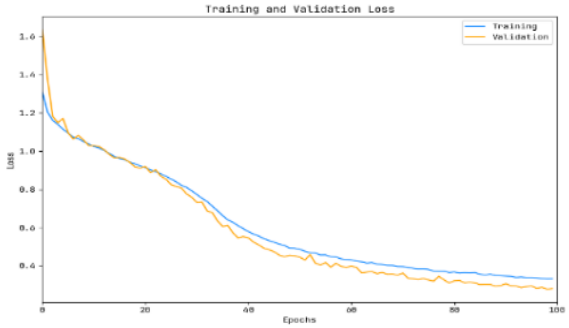

(b)

Figure 18. (a) Accuracy and (b) loss versus number of epochs plot of the 1D CNN-ResNet approach

6.3. Analysis of 1D CNN-ResNet to Categorize Five Classes

The confusion matrix, precision recall curve, roc analysis generated by 1D CNN-ResNet for training data is shown in *figure 19a- figure19c*, indicating accurate identification of all five class labels. Additionally, *figure 20a- figure 20c*, display the confusion matrix, precision recall curve, roc analysis of the classifier on test data.

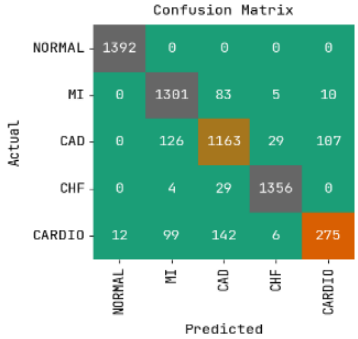

(a)

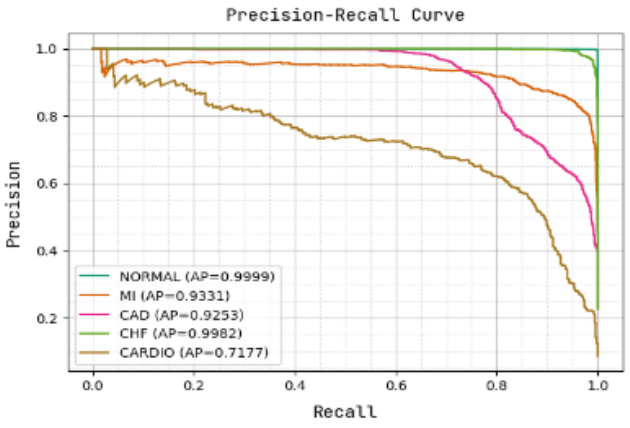

(b)

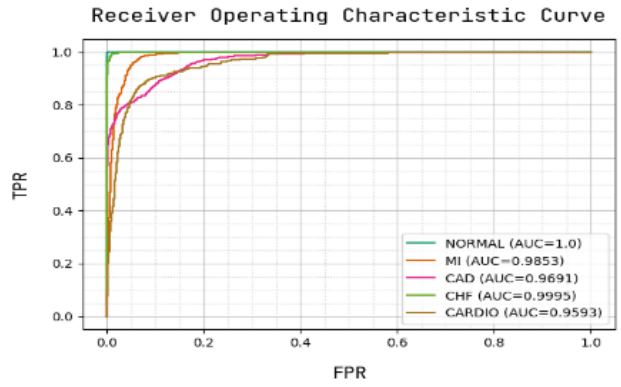

(c)

Figure 19. Training set analysis on 1D CNN-ResNet (a) Confusion matrix (b) PR-curve (c) ROC-curve

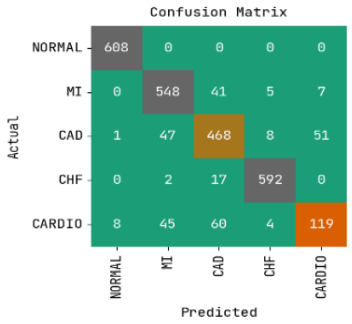

(a)

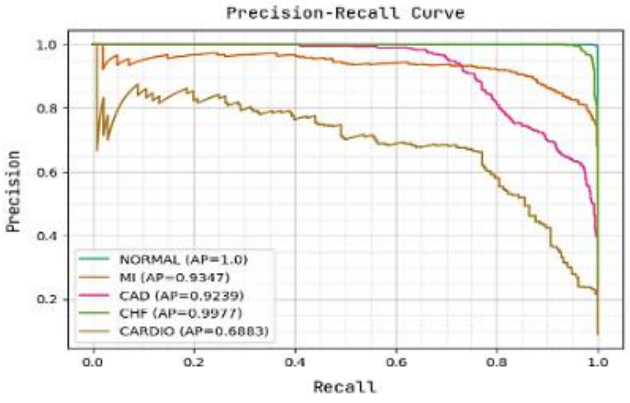

(b)

FOREX Publication
Open Access | Rapid and quality publishing
International Journal of Electrical and Electronics Research (IJEER)
Research Article | Volume 12, Issue 4 | Pages 1301-1323 | e-ISSN: 2347-470X

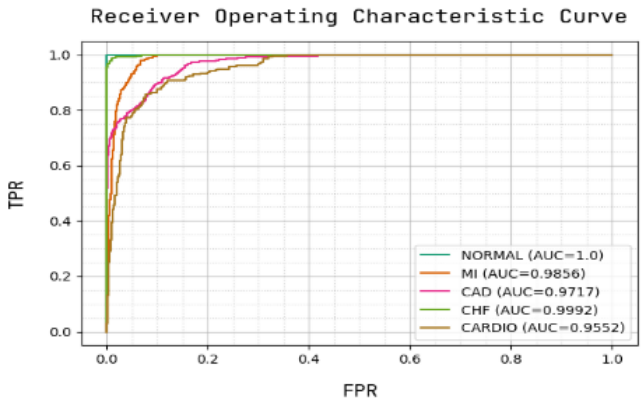

(c)

Figure 20. Testing set analysis on 1D CNN-ResNet (a) Confusion matrix (b) PR-Curve (c) ROC-curve

In *table 7*, the 1D CNN-ResNet technique's ECG classification results are investigated under various classes. The findings show that the approach correctly distinguishes between 5 classes. For instance, on training set the 1DCNN-ResNet technique attains average $accu_y$ of 95.75%, $prec_n$ of 86.71%, $sens_y$ of 84.74%, $spec_y$ of 97.32%, Fscore of 85.41%, and MCC of 82.98%. At the same time, on testing set, the 1DCNN-ResNet technique acquires average $accu_y$ of 95.5%, $prec_n$ of 85.64%, $sens_y$ of 83.98%, $spec_y$ of 97.19%, Fscore of 84.55%, and MCC of 81.94%.

Table 7. Classifier outcome of 1D CNN-ResNet approach with distinct measure in percentage

1D CNN-ResNet (Training Set)						
Class	**Accuracy**	**Precision**	**Sensitivity**	**Specificity**	**F-Score**	**MCC**
NORMAL	99.8	99.15	99.8	99.75	99.57	99.45
MI	94.67	85.03	92.99	95.17	88.84	85.49
CAD	91.59	82.07	81.61	94.61	81.84	76.38
CHF	98.81	97.13	97.62	99.16	97.38	96.61
Cardio	93.88	70.15	51.5	97.91	59.4	56.95
Average	**95.75**	**86.71**	**84.74**	**97.32**	**85.41**	**82.98**
1D CNN-ResNet (Testing Set)						
NORMAL	99.66	98.54	99.5	99.56	99.27	99.05
MI	94.41	85.36	91.18	95.37	88.17	84.6
CAD	91.45	79.86	81.39	94.26	80.62	75.14
CHF	98.63	97.21	96.89	99.16	97.05	96.16
Cardio	93.35	67.23	50.42	97.58	57.63	54.76
Average	**95.5**	**85.64**	**83.98**	**97.19**	**84.55**	**81.94**

Figure 21, investigates the above method's precision while being trained and validated on the test database. It indicates that 50 epochs provide the higher accuracy values. Furthermore, the approach effectively learns at a 0.001 rate from the test database as evidenced by the increased validation accuracy compared to training accuracy. The loss analysis during training and validation on the test database is verified. According to the findings, the approach achieves closer training and validation loss values.

(a)

FOREX Publication
Open Access | Rapid and quality publishing
International Journal of Electrical and Electronics Research (IJEER)
Research Article | Volume 12, Issue 4 | Pages 1301-1323 | e-ISSN: 2347-470X

(b)

Figure 21. (a) Accuracy and (b) loss versus number of epochs plot of the 1D CNN-ResNet approach

Due to the limited study on the use of hybrid DL methods to classify 4 different CAD, MI, CHF and cardiomyopathy ailments, the proposed technique's ECG classification results are contrasted with cotemporary DL models as in Table 8. The 1D CNN-RHNN technique's ECG classification results are contrasted with few hybrid DL models. The result highlighted that the RNN-LSTM model achieves worse results with the least accuracy of 88%. At the same time, the Dense Net-GRU, Ensemble SVM, and Deep residual CNN models have reached slightly closer performance. Meanwhile, the CNN-LSTM and CNN+BiLSTM models have reported moderately improved results. Furthermore, the 1DCNN-RHNN technique has outperformed the existing models with a maximum of 96.62% accuracy.

Table 8. Comparison of outlined approach with other contemporary hybrid DL approaches

Author	Dataset	DL Approach	Type of Subject	Average Accuracy (%)
Shahid AH et al. [9]	Z-Alizadeh Sani dataset 303 subjects	Hybrid Particle swarm optimization (PSO) based emotional neural network (EmNN)	CAD, MI, Normal	88.34
Hasan NI et al. [10]	MIT-BIH- 4 classes, PTB database-7 classes and St.-Petersburg- 9 classes	Empirical mode decomposition 1DCNN 10-fold validation	4 arrhythmia types CAD, MI, CHF, cardiomyopathy and multiple CVDs	PTB - 98.24 MIT-BIH - 97.70 St.-Petersburg- 99.7
Rai H M et al. [12]	PTBDB –MI MITDB - normal	CNN-LSTM 10-fold validation	MI and normal	99
Rath A et al. [13]	MIT-BIH and PTBDB	Generative adversarial network - LSTM	Arrhythmia	99.2 99.4
Malik J et al. [14]	MIT-BIH mapped to AAMI heart beat types	1D Self-ONNs Self-operational neural network Patient Specific	Non ectopic (N) supraventricular ectopic (SVEB), ventricular ectopic (VEB), fusion beat (F), unknown beats (Q)	SVEB- 98 VEB-99
Abdar M et al. [15]	Z-Alizadeh Sani dataset	Genetic algorithm and PSO – feature selection, N2 Genetic optimizer-nuSVM	CAD and Normal	93
Butun E et al. [16]	St.-Petersburg (INCARTDB)- CAD Fantasia database-normal	1D version of Capsule Network 5-fold validation	CAD and Normal	99
Jahmunah V et al. [17]	Fantasia database-normal St Petersburg (INCARTDB) - CAD, PTBDB - MI, and BIDMC - CHF - CHF	Gabor-CNN 10-fold validation	Normal, CAD, MI, and CHF	98.74
Petmezas G et al. [18]	MIT-BIH Atrial Fibrillation	1D CNN – LSTM 10-fold validation	Normal (N), atrial fibrillation (AFIB), atrial flutter (AFL) and AV junctional rhythm (J)	Sensitivity – 97.87 Specificity – 99.29
Lih O S et al. [19]	Phsionet.org	1D CNN – LSTM 10-fold validation	Normal, CAD, MI, and CHF	98

Xue Xu et al. [21]	MIT-BIH mapped to AAMI heart beat types	1D CNN - BiLSTM	N, SVEB, VEB, F, Q 5 arrhythmia beat types	95.90
Balaji G N et al. [22]	Echocardiogram video	fuzzy C-means clustering and morphological operations linear discriminant analysis, K-nearest neighbor, Hopfield neural network	Normal and Dilated Cardiomyopathy	LDA - 84 K-NN - 74 HNN - 88
Anand R et al. [23]	MIT-BIH Database	1-D CNN ResNet-18	N, SVEB, VEB, F, Q 5 arrhythmia beat types	1D – CNN – 97.86 R ResNet-18 - 99
Nizar Sakli et al. [24]	MIT-BIH Database	ResNet-50	27 arrhythmia types	97
Guo L et al. [26]	MIT-BIH Database	Dense Net – Gated Recurrent Unit (GRU)	Normal (N), supraventricular ectopic (SVEB), ventricular ectopic (VEB), fusion beat (F)	92 %
Essa E et al. [27]	MIT-BIH Database	CNN-LSTM	N, SVEB, VEB, F 4 arrhythmia beat types	96 %
Kachuee M et al. [28]	MIT-BIH Database PTBDB	Deep residual CNN	Arrhythmia and MI beat	93 / 96 %
Clement Virgeniya S et al. [29]	PTB-XL dataset	CIGRU-ELM Adaptive Synthetic data sampler	Normal ECG, conduction disturbance,myocardial infarction, hypertrophy and ST/T changes	87
Khan F et al. [30]	Physio Net MIT-BIH Arrhythmia database	1-D convolutional deep residual neural network with SMOTE 10-fold validation	N, SVEB, VEB, F, Q 5 arrhythmia beat types	98.63
Singh et al. [31]	MIT-BIH Database	Ensemble of support vector machine (SVM)	N, SVEB, VEB, F 4 arrhythmia beat types	93%
Singh et al. [32]	MIT-BIH Database PTBDB	RNN-LSTM	Normal and Abnormal beat	88%
Guo L et al. [33]	International Cooperation Center of Xining Hospital 423 subjects	least absolute shrinkage selection operator (LASSO) logistic regression (LR)	Hypertrophic cardiomyopathy (HCM) and Non HCM	Promising results
Dey M et al. [34]	Physio bank (PTB) ECG database	1D CNN - BiLSTM	Heart Conduction, MI, and non-myocardial infarction	99
Hao dai et al. [35]	Physio bank (PTB) ECG database	min-max normalization 1D CNN	MI, hypertrophy cardiomyopathy, (HCM),Dilated cardiomyopathy (DCM), normal, Valvular heart disease (VHD), Bundle branch block (BBB)	1s ECG – 99.59 2s ECG – 99.87 3s ECG – 99.93
Lianke Yao et al., [36]	Shandong Provincial Qian Foshan Hospital 93 CAD 107 normal	ResNet-18 XG Boost RR and QT interval time-series features	Normal and CAD	96.16
Yang, W et al. [37]	MIT-BIH Normal Sinus Rhythm Database (NSRDB) St Petersburg (INCARTDB) BIDMC - CHF	ECG fragment alignment (EFA)-principal component analysis (PCA) convolutional network (EFAP-Net). linear support vector machine 10-fold cross validation	Datasets A (normal+CAD), B (normal+CHF), C (normal+CAD+CHF)	A - 99.84 B - 99.92 C- 99.80
Wang, Z et al. [38]	PTB MI ECG	PCA features, statistical features, entropy features, Ensemble classifier, SVM, K-NN, Random Forest	Normal and MI	intra-patient scheme 99.71 inter-patient classification 85.82
Prabhakararao, E et al. [39]	PTBDB	recurrent neural network with intra- and inter-lead attention modules	MI, Non MI and HC	98.3

International Journal of Electrical and Electronics Research (IJEER)
Research Article | Volume 12, Issue 4 | Pages 1301-1323 | e-ISSN: 2347-470X

Xiong P et al. [40]	PTBDB	Dense Net 10-fold cross validation	Normal, MI and MI types	99.87
Riek NT et al. [41]	PTBDB	Residual CNN	Occlusion MI detection (OMI)	94.7
Alaa Eleyan et al. [42]	MIT-BIH BIDMC	CNN - LSTM	N, SVEB, VEB, F, Q CHF	97 99
Nikhat Parveen et al. [43]	MIT-BIH arrhythmia dataset	1D Residual Deep Convolutional Auto-Encoder (1D-RDCAE) + extreme gradient boosting (XGB) SMOTE – data balancing	N – normal P – paced rhythms LBBB – left bundle branch block PVC – premature ventricular contraction RBBB – right bundle branch block	99.6
Haobo Zhang et al. [44]	PhysioNet CinC Challenge 2016 dataset	Co-learning-assisted Progressive Dense fusion network (CPD Net) 5-fold validation	Normal and CVDs (abnormal)	94
Aarthy ST et al. [45]	specific dataset from SRM College Hospital and Research Centre	AlexNet50 fuzzy bi-clustering approach	AF, CHF and NSR	98
Immaculate Joy S et al. [46]	PTB-XL dataset 21,799 ECGs from 18,869 patients	CNN + Variational Auto encoder (VAE)	Normal sinus rhythm, MI, Conduction disturbance (CD), ST/T Change (STTC), Hypertrophy (HYP)	98.5
Revathi T K et al. [47]	Cleveland heart disease dataset	Optimally Configured and Improved Long Short-Term Memory (OCI-LSTM) Salp Swarm Algorithm, Genetic Algorithm	Normal and abnormal class using attributes	97
Biao Xia et al.[48]	Kaggle Repository Healthy – 561 Diseased - 629	Intelligent Cardiovascular Disease Diagnosis based on Ant Colony Optimization with Enhanced Deep Learning (ICVD-ACOEDL)	Prepared medical dataset using attributes Healthy and diseased	97
David Opeoluwa Oyewola et al. [49]	Kaggle cardiovascular data set 12 attributes 70,000 instances	LSTM (long short-term memory) FFNN (feed forward neural network) ELMAN (Elman neural network) CFNN (cascade forward neural network) EDL (ensemble deep learning)	Diseased and Healthy label based	98
Chaoqun Guo et al. [50]	PhysioNet MIT-BIH Arrhythmia database - AAMI	SMOTE Multiscale Convolutional Neural Network Convolutional Causal Attention Network 5-fold validation	N, SVEB, VEB, F, Q	99
Proposed	PTBDB- MI, normal, cardiomyopathy St. Petersburg (INCARTDB) – CAD BIDMC-CHF- CHF Fantasia database- normal Lead- II ECG segments	1D CNN with RHNN 1D CNN with ResNet 1D CNN with ResNet	Normal, CAD, MI, CHF Normal, CAD, MI, CHF Normal, CAD, MI, CHF, and Cardiomyopathy	96.6 92.8 95.7

The findings say that many kinds of DL strategies are used to detect CVDs. Several perceptions were made:
1. Several others used the single DL way to figure out only just one CVD.
2. Some applied the mixed DL way to identify a single form of CVD, especially CAD, CHF, MI, or Cardiomyopathy.
3. Several of them presented an integrated plan to sort many kinds of ailments, but nearly all of them relied on arrhythmias.
4. There has been very little investigation on incorporating a combination of DL techniques for evaluating several CVDs notably CAD, MI, CHF, and cardiomyopathy. In this instance are the positive effects of one's work: The 1D CNN-RHNN technique has outperformed with a maximum accuracy of 96.62% in detecting CAD, MI, CHF and normal class, 1D CNN-ResNet technique reported an accuracy of 92.84% in detecting CAD, MI, CHF and normal class and the same showed an accuracy of 95.75% in detecting CAD, MI, CHF, cardiomyopathy and normal class.

The chief limitation of this investigation is that the frameworks were not developed and assessed adopting the complete 1, 39, 795 sample populations pool of Physio Net. Merely selected segments picked at random have been use to evaluate each of the stated methods. To boost reliability of classification, we are anticipating using the acquired all of the data portions for validation and training of the blended learning process. Moreover, we intend to put in a 10-fold cross validation approach to fortify the frameworks. However, the study's reliance on datasets from physionet.org may limit its representation of real-world variability. Further validation and integration into hospital systems are necessary to assess the clinical applicability of the developed model. Nonetheless, the study's data balancing technique effectively improved accuracy for CVDs detection. Nevertheless, limitations of the study include data variability, limited interpretability, and inadequate discussion on real-time data implementation. Further in future investigations and improvements are necessary to address these limitations and establish the practical viability of the proposed approach. DL applicability for healthcare may be enhanced by interactions involving studies, physicians, along with information analysts.

7. CONCLUSION

In order to detect problems with the heart, the ECG readings are vital. The sort of defects can be made more accurately with modelling than with hands-on techniques. In this article, an automated CVD classification model has been developed. The purpose of the proposed model is to utilize hybrid DL models to accurately detect various types of CVD. The presented model leverages the power of CNN, RNN, and ResNet for the extraction of related features from ECG signals and classifies them into various classes corresponding to specific CVD conditions. Initially the 1D CNN with ResNet is built, trained, and validated to categorise four different classes later the 1D CNN with RHNN is constructed to classify among four classes. Further the two hybrid DL model developed are examined to classify among five different group. This process attempts anticipate both conventional & minor changes in heartbeat sequences, these then correspond on a built attribute group of CVDs. On comparing all detected characteristics toward built-in CVD sequences, experts may correlate every tiny difference with one's cardiac wellness. The design of these models for ECG classification offers an effective approach to diagnosing multiple CVDs. On a large collection of ECG datasets, the suggested method's widely used simulation result analysis is put to the test, and the results are examined in terms of a number of metrics. When compared to independent DL models and conventional ECG classification methods, the provided model performs better when multiple CVDs are considered. The suggested model can use the feature selection strategy in the future to enhance the performance of ECG classification. Other data matching methods can be applied to produce replica datasets then contrast findings over the overall originally collected data.

Author Contributions: Conceptualization, methodology, software, writing—original draft preparation, Padmavathi C.; writing—review and editing, supervision, Veenadevi S V. All authors have read and approved the final version of the manuscript.

Funding Source: This research received no external funding

Acknowledgments: We would like to express our gratitude to the reviewers for their suggestions that improved the presentation of the results obtained.
Conflicts of Interest: No conflict of interest to declare.

REFERENCES

[1] World Health Organization (WHO). Cardiovascular Diseases (CVDs), https://www.who.int/news-room/fact-sheets/detail/cardiovascular-diseases-(cvds). [Accessed: Jun. 11, 2021].

[2] Hu, R.; Chen, J.; Zhou, L. A transformer-based deep neural network for arrhythmia detection using continuous ECG signals. Computers in Biology and Medicine. 2022, vol. 144, 105325.

[3] Hammad, M.; Chelloug, S.A.; Alkanhel, R.; Prakash, A.J.; Muthanna, A.; Elgendy, I.A.; Pławiak, P. Automated detection of myocardial infarction and heart conduction disorders based on feature selection and a deep learning model. Sensors. 2022, vol. 22, no. 17, 6503.

[4] Nguyen, J.T.; Li, X.; Lü, F. The electrocardiogram and clinical cardiac electrophysiology. Cardiac Electrophysiology Methods and Models. Springer, Boston, MA. 2010, pp. 91-116.

[5] Peterkova, A.; Stremy, M. The raw ECG signal processing and the detection of QRS complex. IEEE European modelling symposium, 2015, pp.80-85.

[6] Siontis, K.C.; Noseworthy, P.A.; Attia, Z.I.; Friedman, P.A. Artificial intelligence-enhanced electrocardiography in cardiovascular disease management. Nature Reviews Cardiology. 2021, vol.18, no.7, pp.465-478.

[7] Davenport, T.; Kalakota, R. The potential for artificial intelligence in healthcare. Future Healthcare Journal. 2019, vol. 6, no.2, pp.94-98.

[8] Liu, X.; Wang, H.; Li, Z.; Qin, L. Deep learning in ECG diagnosis: A review. Knowledge-Based Systems. 2021, vol.227, pp. 107-187.

[9] Shahid, A.H.; Singh, M.P. A novel approach for coronary artery disease diagnosis using hybrid particle swarm optimization based emotional neural network. Biocybernetics and Biomedical Engineering. 2020, vol. 4, no.4, pp.1568-1585.

[10] Hasan, N.I.; Bhattacharjee, A. Deep learning approach to cardiovascular disease classification employing modified ECG signal from empirical mode decomposition. Biomedical Signal Processing and Control. 2019, vol.52, pp. 128-140.

[11] Fatema, K.; Montaha, S.M.; Rony A.H.; Azam, S.; Hasan M.Z.; Jonkman, M.A. Robust Framework Combining Image Processing and Deep Learning Hybrid Model to Classify Cardiovascular Diseases Using a Limited Number of Paper-Based Complex ECG Images. Biomedicines. 2022, vol.10, no.11, 2835.

[12] Rai, H.M.; Chatterjee, K. Hybrid CNN-LSTM deep learning model and ensemble technique for automatic detection of myocardial infarction using big ECG data. Applied Intelligence. 2022, vol.52, no.5, pp. 5366 - 5384.

[13] Rath, A.; Mishra, D.; Panda, G.; Satapathy, S.C. Heart disease detection using deep learning methods from imbalanced ECG samples. Biomedical Signal Processing and Control. 2021, 68, 102820.

[14] Malik, J.; Devecioglu, O.C.; Kiranyaz, S.; Ince, T.; Gabbouj, M. Real-Time Patient-Specific ECG Classification by 1D Self-Operational Neural Networks. IEEE Transactions on Biomedical Engineering. 2022, vol.69, no.5, pp.1788-1801.

[15] Abdar, M.; Książek, W.; Acharya, U.R.; Tan, R.S.; Makarenkov, V.; Pławiak, P. A new machine learning technique for an accurate diagnosis of coronary artery disease. Computer Methods and Programs in Biomedicine. 2019, vol. 179, 104992.

[16] Butun, E.; Yildirim, O.; Talo, M.; Tan, R.S.; Rajendra Acharya U. 1D-CADCapsNet: One dimensional deep capsule network for coronary artery disease detection using ECG signals. Phys Med. 2020, vol. 70, pp. 39-48.

[17] Jahmunah, V.; Ng E.Y.K.; San T.R.; Acharya U.R. Automated detection of coronary artery disease, myocardial infarction, and congestive heart failure using Gabor CNN model with ECG signals. Computers in Biology and Medicine, 2021, vol.134, 104457.

[18] Petmezas, G.; Haris, K.; Stefanopoulos, L.; Kilintzis, V.; Tzavelis, A.; Rogers, J.A.; Katsaggelos A.K.; Maglaveras, N. Automated Atrial Fibrillation Detection using a Hybrid CNN-LSTM Network on Imbalanced ECG Datasets. Biomedical Signal Processing and Control. 2021, vol.63, 102194.

[19] Lih Oh Shu.; Jahmunah, V.; San, T.R.; Ciaccio, E.J.; Yamakawa, T.; Tanabe, M.; Kobayashi, M.; Faust, O.; Acharya, U.R. Comprehensive electrocardiographic diagnosis based on deep learning. Artificial Intelligence in Medicine. 2020, vol. 103, 101789.

[20] Zhang, X.; Gu, K.; Miao, S.; Yin, Y.; Wan, C.; Yu, Y.; Hu, J.; Wang, Z.; Shan, T.; Jing, S.; Wang, W.; Ge, Y.; Chen, Y.; Guo, J.; Liu, Y. Automated detection of cardiovascular disease by electrocardiogram signal analysis: a deep learning system. Cardiovascular Diagnosis and Therapy. 2020, vol.10, no. 2, pp. 227-235.

[21] Xu, X.; Jeong, S.; Li, J. Interpretation of Electrocardiogram (ECG) Rhythm by Combined CNN and BiLSTM. IEEE Access. 2020, vol. 8, pp. 125380-125388.

[22] Balaji, G.N.; Subashini, T.S.; Suresh, A.; Prashanth, S. Detection and diagnosis of dilated cardiomyopathy from the left ventricular parameters in echocardiogram sequence. International Journal of Biomedical Engineering and Technology. 2019, vol. 31, no. 4, pp. 346–364.

[23] Anand, R.; Vijaya Lakshmi, S.; Digvijay Pandey; Binay Kumar Pandey. An enhanced ResNet 50 deep learning model for arrhythmia detection using electrocardiogram biomedical indicators. Evolving Systems. 2024, vol. 15, no.1, pp.1-15.

[24] Nizar Sakli; Haifa Ghabri; Ben Othman Soufiene; Faris. A.; Almalki; Hedi Sakli; Obaid Ali; Mustapha Najjari. ResNet-50 for 12-Lead Electrocardiogram Automated Diagnosis. Computational Intelligence and Neuroscience. 2022, DOI: 10.1155/2022/7617551.

[25] Kingma, D.P.; Ba, J. Adam: A Method for Stochastic Optimization. 2015, pp.1–15. https://doi.org/10.48550/arXiv.1412.6980.

[26] Guo, L.; Sim, G.; Matuszewski, B. Inter-patient ECG classification with convolutional and recurrent neural networks. Biocybernetics and Biomedical Engineering. 2019, vol.39, no. 3, pp.868-879.

[27] Essa, E.; Xie, X. An ensemble of deep learning-based multi-model for ECG heartbeats arrhythmia classification. IEEE Access. 2021, vol. 9, no.1, pp. 103452-103464.

[28] Kachuee, M.; Fazeli, S.; Sarrafzadeh, M. ECG heartbeat classification A deep transferable representation. 2018 IEEE International Conference on Healthcare Informatics, ICHI 2018, New York, NY, USA, pp.443–444.

[29] Clement Virgeniya, S.; Ramaraj, E. A Novel Deep Learning based Gated Recurrent Unit with Extreme Learning Machine for Electrocardiogram (ECG) Signal Recognition. Biomedical Signal Processing and Control. 2021, vol.68, 102779.

[30] Khan, F.; Yu, X.; Yuan, Z.; Rehman Au. ECG classification using 1-D convolutional deep residual neural network. PLoS ONE. 2023, vol.18, no. 4, e0284791.

[31] Singh, V.; Reddy, US.; Bhargavia, GM. A Generic and Robust System for Automated Detection of Different Classes of Arrhythmia. Procedia Computer Science. 2020, vol. 167, pp. 1801-1810.

[32] Singh, S.; Pandey, SK.; Pawar, U.; Janghel, RR. Classification of ECG arrhythmia using recurrent neural networks. Procedia Comput. Sci. 2022, vol. 132, pp. 1290-1297.

[33] Guo, L.; Gao, C.; Yang, W.; Ma, Z.; Zhou, M.; Liu, J.; Shao, H.; Wang, B.; Hu, G.; Zhao, H.; Zhang, L.; Guo, X.; Huang, C.; Cui, Z.; Song, D.; Sun, F.; Liu, L.; Zhang, F.; Tao, L. Derivation and Validation of a Screening Model for Hypertrophic Cardiomyopathy Based on Electrocardiogram Features. Frontiers in Cardiovascular Medicine. 2022, 9:889523. doi: 10.3389/fcvm.2022.889523.

[34] Dey, M.; Omar, N.; Ullah, M.A. Temporal Feature-Based Classification into Myocardial Infarction and Other CVDs Merging CNN and Bi-LSTM from ECG Signal. IEEE Sensors Journal. 2021, vol. 21, no. 19, pp. 21688-21695, doi: 10.1109/JSEN.2021.3079241.

[35] Hao Dai.; Hsin-Ginn.; Hwang.; Vincent, S.; Tseng. Convolutional neural network based automatic screening tool for cardiovascular diseases using different intervals of ECG signals, Computer Methods

International Journal of Electrical and Electronics Research (IJEER)
Research Article | Volume 12, Issue 4 | Pages 1301-1323 | e-ISSN: 2347-470X

and Programs in Biomedicine, 2021, vol. 203, 106035, ISSN 0169-2607, https://doi.org/10.1016/j.cmpb.2021.106035.

[36] Yao, L.; Liu, C.; Li, P.; Wang, J.; Liu, Y.; Li, W.; Wang, X.; Li, H.; Zhang, H. Enhanced automated diagnosis of coronary artery disease using features extracted from QT interval time series and ST–T waveform, IEEE Access, 2020, vol.8, 129510–129524, https://doi.org/10.1109/ACCESS.2020.3008965.

[37] Yang, W.; Yujuan Si.; Di Wang.; Zhang, G.; Xin Liu.; Liang Liang Li. Automated intra-patient and inter-patient coronary artery disease and congestive heart failure detection using EFAP-Net. Knowledge-Based Systems, 2020, vol. 201–202, 106083, ISSN 0950-7051.

[38] Zhizhong Wang.; Longlong, Qian,; Chuang Han, et ao.; Li Shi.Application of multi-feature fusion and random forests to the automated detection of myocardial infarction, Cognitive Systems Research, 2020, vol. 59, pp. 15-26, ISSN 1389-0417,

[39] Prabhakararao, E.; Dandapat. S. Attentive RNN-Based Network to Fuse 12-Lead ECG and Clinical Features for Improved Myocardial Infarction Diagnosis. IEEE Signal Processing Letters, 2020, vol. 27 pp.2029-2033.

[40] Xiong, P.; Xue, Y.; Zhang, J.; Liu, M.; Du, H.; Zhang, H.; Hou, Z.; Wang, H.; Liu, X. Localization of myocardial infarction with multi-lead ECG based on DenseNet. Computer methods and programs in biomedicine, 2021, 203, 106024.

[41] Riek, NT., Akcakaya, M.; Bouzid, Z.; Gokhale, T.; Helman, S.; Kraevsky-Philips, K.; et al. ECG-SMART-NET: a deep learning architecture for precise ECG diagnosis of occlusion myocardial infarction. 2024.

[42] Eleyan, A.; Alboghbaish, E. Electrocardiogram Signals Classification Using Deep-Learning-Based Incorporated Convolutional Neural Network and Long Short-Term Memory Framework. Computers. 2024, 13, 55. https://doi.org/10.3390/computers13020055.

[43] Parveen, N.; Gupta, M.; Kasireddy, S. et al. ECG based one-dimensional residual deep convolutional auto-encoder model for heart disease classification. Multimedia Tools and Applications. 2024, 83, 66107–66133. https://doi.org/10.1007/s11042-023-18009-7.

[44] Haobo Zhang.; Peng Zhang.; Fan Lin.; Lianying Chao.; Zhiwei Wang.; Fei Ma.; Qiang Li. Co-learning-assisted progressive dense fusion network for cardiovascular disease detection using ECG and PCG signals, Expert Systems with Applications, 2024, vol. 238, 122144, ISSN 0957-4174, https://doi.org/10.1016/j.eswa.2023.122144.

[45] Aarthy, S T.; Mazher Iqbal, J L. A novel deep learning approach for early detection of cardiovascular diseases from ECG signals, Medical Engineering & Physics, 2024, vol. 125, 104111, ISSN 1350-4533, https://doi.org/10.1016/j.medengphy.2024.104111.

[46] Immaculate Joy, S.; Moorthi, M.; Senthil Kumar, K. Detection and Classification of electrocardiography using hybrid deep learning models, Hellenic Journal of Cardiology, 2024, ISSN 1109-9666, https://doi.org/10.1016/j.hjc.2024.08.011.

[47] Revathi, T.K.; Balasubramaniam, S.; Sureshkumar, V.; Dhanasekaran, S. An Improved Long Short-Term Memory Algorithm for Cardiovascular Disease Prediction. Diagnostics, 2024, 14, 239. https://doi.org/10.3390/diagnostics14030239.

[48] Xia, B.; Innab, N.; Kandasamy, V. et al. Intelligent cardiovascular disease diagnosis using deep learning enhanced neural network with ant colony optimization. Scientific Reports, 2024, 14, 21777. https://doi.org/10.1038/s41598-024-71932-z.

[49] David Opeoluwa Oyewola.; Emmanuel Gbenga Dada.; Sanjay Misra. Diagnosis of Cardiovascular Diseases by Ensemble Optimization Deep Learning Techniques. International Journal of Healthcare Information Systems and Informatics, 2024, vol.19, no.1. https://doi.org/ 10.4018/IJHISI.334021.

[50] Guo C.; Yin B.; Hu J. An Electrocardiogram Classification Using a Multiscale Convolutional Causal Attention Network. Electronics. 2024, vol. 13, no. 2, 326. https://doi.org/10.3390/electronics13020326.